RNA LIGATION BY HAMMERHEAD RIBOZYMES AND DNAZYME IN PLAUSIBLE PREBIOTIC CONDITIONS

A Dissertation
Presented to
The Academic Faculty

by

Lively Lie

In Partial Fulfillment
of the Requirements for the Degree
Doctor of Philosophy in the
School of Biology

Georgia Institute of Technology
DECEMBER 2015

RNA LIGATION BY HAMMERHEAD RIBOZYMES AND DNAZYME IN PLAUSIBLE PREBIOTIC CONDITIONS

Approved by:

Dr. Roger M. Wartell, Advisor
School of Biology
Georgia Institute of Technology

Dr. Eric Gaucher
School of Biology
Georgia Institute of Technology

Dr. Loren D. Williams
School of Chemistry & Biochemistry
Georgia Institute of Technology

Dr. Fredrik Vannberg
School of Biology
Georgia Institute of Technology

Dr. Nicholas Hud
School of Chemistry & Biochemistry
Georgia Institute of Technology

Date Approved: August 13, 2015

ACKNOWLEDGEMENTS

First, I would like to thank my family. Without the support of my mother and father, I would not have reached this far. To my husband, I thank him for his patience, love, and his knowledge of programming and computers. I would also like to thank the undergraduate students Rachel Hutto, Philip Kaltman, and Audrey Calvird who contributed to the research in this thesis and the lab technicians Eric O'Neill, Jessica Bowman, and Shweta Biliya, who seemed to know the answers to my troubleshooting. Finally, many thanks goes to my advisor Dr. Roger Wartell, always a helpful, patient, and kind mentor.

TABLE OF CONTENTS

	Page
ACKNOWLEDGEMENTS	iv
LIST OF TABLES	vii
LIST OF FIGURES	viii
LIST OF SYMBOLS AND ABBREVIATIONS	xi
SUMMARY	xii
CHAPTER	
1 Introduction	1
RNA World Hypothesis	2
Potential Role of Fe^{2+} in RNA Catalysis	2
Ribozymes Perform a Variety of Functions	3
Challenges to the RNA World Hypothesis	4
Hammerhead Ribozyme	8
DNAzymes in the RNA World	10
Summary of Thesis	11
2 Effect of Fe^{2+} on Hammerhead Catalysis	14
Introduction	14
Materials and Methods	19
Results	21
Discussion	24
3 Hammerhead Ribozyme Ligation in Ice	26
Introduction	26
Materials and Methods	31

Results 33
Discussion 47
Supplementary 50
4 Effect of Mutant P1 and P2 on Hammerhead Ligation in Ice 52
Introduction 52
Materials and Methods 54
Results 57
Discussion 61
Supplementary 62
5 DNAzyme Ligation in Ice 68
Introduction 68
Materials and Methods 71
Results 72
Discussion 75
6 Conclusion 76
Growing the Ribosomal RNA 76
REFERENCES 82
VITA 90

LIST OF TABLES

Table S4.1: Top 100 most frequent sequences from the Illumina Hiseq runs of Schist26 ligation with P2-5N. 62

Table 5.1: Dinucleotide junctions with associated DNAzyme/RNA substrate pair. 73

LIST OF FIGURES

Page

Figure 1.1: The Central Dogma as was known in 1970, with solid lines indicating probable transfers and dashed lines as possible transfers. 1

Figure 1.2: QM models for RNA-Mg^{2+} and RNA-Fe^{2+} clamps. 3

Figure 1.3: Phase diagram of NaCl with variable temperature and salt concentration. 5

Figure 1.4: Electron Microscopy images of ice surrounding channels containing the eutectic phase. 6

Figure 1.5: Simplified model of Round 18 ligase and its protection from degradation in ice. 7

Figure 1.6: Truncated forms of the Hairpin ribozyme. 8

Figure 1.7: Disulfide crosslinker between Stems I and II increase HHα1 hammerhead ligation activity. 9

Figure 1.8: Secondary structure model of the Schist26 Hammerhead ribozyme. 10

Figure 1.9: Secondary structure model of 8-17 and 10-23 dnazyme catalytic cores and binding arms. 11

Figure 2.1: Similar conformations between the RNA-Mg^{2+} and RNA-Fe^{2+} clamps based on QM calculations. 13

Figure 2.2: SHAPE footprinting of the P4-P6 domain of the *Tetrahymena thermophila* Group I intron. 15

Figure 2.3: Fe^{2+} induced ligation of the L1 ligase shows a 25-fold higher initial rate of ligation than with Mg^{2+}. 16

Figure 2.4: Secondary structure of truncated HHα1 hammerhead and Schist26 hammerhead. 17

Figure 2.5: Mn^{2+} coordination of the scissile phosphate in the active site of the hammerhead ribozyme. 18

Figure 2.6: Hammerhead ribozyme cleavage is enhanced in Fe^{2+} compared to Mg^{2+}. 21

Figure 2.7: Enhanced Fe^{2+}-induced ligation by the Schist26 hammerhead ribozyme at 25 °C. 22

Figure 3.1: Secondary structure of minimal hammerhead ribozyme. 26

Figure 3.2: Single turnover ligation reaction of Schist26 over the course of 18 seconds. 28

Figure 3.3: Schist26 hammerhead ribozyme with labeled stems. 29

Figure 3.4: Single turnover ligation kinetics of ^{32}P labeled P1>p and P2 oligomer catalyzed by the hammerhead ribozyme at 25 °C. 33

Figure 3.5: 20% PAGE of ^{32}P-P1>p in the presence of 10 mM $MgCl_2$ at room temperature. 34

Figure 3.6: 12 % denaturing polyacrylamide gel showing ligation of P1>p to P2 by the hammerhead ribozyme under freezing conditions. 36

Figure 3.7: Cleavage of the full length substrate by the Schist26 hammerhead in frozen NTE buffer. 37

Figure 3.8: 12% PAGE of dehydration-induced ligation of ^{32}P-P1•P2. 38

Figure 3.9: Single turnover ligation reaction of the Schist26 hammerhead in 4M NaCl at 25 °C. 40

Figure 3.10: Effects of substituting different cations and sodium salt anions for the 100 mM NaCl of the standard NTE solution on the fraction of ligated P1>p. 41

Figure 3.11: Thermal cycling on Hammerhead ribozyme ligation. 43

Figure 3.12: pH measurement of various buffers before and during freezing at -20 °C. 45

Figure S3.1: Reaction scheme of the Schist26 HHR reversible cleavage and ligation reaction with a branching irreversible side reaction for P1-p. 49

Figure S3.2: Proposed mechanism for hammerhead ligation with a carboxylate participating in the acid/base chemistry during catalysis. 50

Figure S3.3: Plot Percent Ligated by Schist26 hammerhead versus Jones-Dole viscosity B coefficients. 51

Figure 4.1: Secondary structure of the Schist26 hammerhead ribozyme from *Schistosoma mansoni* with its ligation substrates P1 and P2. 54

Figure 4.2: Hammerhead ribozyme ligation using various P1 constructs. 58

Figure 4.3: Visual representation of P2-5N sequences by observed Hiseq frequency. 59

Figure 4.4: Fraction of P1>p ligated to wild type P2 or P2-GG-UGU induced by freezing to -20 °C with sodium citrate, after multiple thermal cycles. 59

Figure 4.5: Comparison of Mg^{2+} induced ligation reaction with mutant P2 at 25 °C in NTE solution with 5 mM Mg^{2+}. 60

Figure S4.1: Perl script used to search for P1•P2-5N from the Hiseq runs. 66

Figure 5.1: RNA Cleavage products catalyzed by both ribozymes and DNAzymes. 69

Figure 5.2: RNA-ligating DNAzyme with a 40 nt core region with binding arms for the two RNA substrates. 70

Figure 5.3: Secondary structure of 8-17 and 10-23 DNAzyme motif. 70

Figure 5.4: DNAzyme motif 10-23 ligating P1>p and P2 RNA of the Schist26 hammerhead ribozyme. 73

Figure 5.5: Plot of 10-23 DNAzyme ligation at different buffer conditions, frozen at -15 °C. 74

Figure 6.1: Model of the a-PTC. 77

Figure 6.2: Ribosomal RNA evolution with insertion fingerprints and ancestral expansion segments (AES). 78

Figure 6.3: Predicted duplex formation of O1 and O2 RNA oligos. 79

Figure 6.4: 12% PAGE replicating the non-enzymatic recombination of RNA oligos done by Lutay et al. 2007. 79

Figure 6.5: Non-enzymatic RNA recombination of AES 1 to include AES 2. 80

Figure 6.6: AES 2 ligating into AES 1 by DNAzymes. 81

LIST OF SYMBOLS AND ABBREVIATIONS

A	Adenine
bp	base pair
C	Cytosine
DNA	Deoxyribonucleic acid
DNAzyme	Deoxyribonucleic acid enzyme
EDTA	ethylene-diamine-tetra-acetic acid
G	Guanine
HEPES	4-(2-hydroxyethyl)-1-piperazineethanesulfonic acid
µM	micromolar
mM	millimolar
M	Molar
nt	nucleotide
PIPES	piperazine-N,N′-bis(2-ethanesulfonic acid)
ribozyme	ribonucleic acid enzyme
rRNA	ribosomal RNA
RNA	Ribonucleic acid
Schist26	*Schistosoma mansoni* hammerhead with a 26 nucleotide cleavage substrate
SHAPE	Selective 2'-hydroxyl acylation analyzed by primer extension
T	Thymine
Tris	Tris(hydroxymethyl)aminomethane
U	Uracil
QM	Quantum mechanical

SUMMARY

This work is focused on the ligation activity of the hammerhead ribozyme and DNAzymes in plausible prebiotic conditions. Before the Great Oxidation Event, RNA may have interacted with soluble Fe^{2+}, as a replacement or in combination with Mg^{2+}. Divalent metal cations are sometimes necessary in ribozyme activity by interacting with mostly phosphates to influence the tertiary structure of an RNA. In some cases, these metal cations help in the acid/base chemistry in catalytic cores.

Chapter 2 reveals the benefits and drawbacks of hammerhead ribozyme ligation with Fe^{2+}. Both ligation and cleavage of the hammerhead is enhanced, but an unexpected problem arose, RNA aggregation that is difficult to denature.

Chapter 3 and 4 focuses on the hammerhead ligation in ice. Freeze-induced ligation frees the hammerhead from divalent metal requirements and when combined with heat-freeze cycles to mimic day and night, yield reaches 60%. Freezing the reaction mixture also reduces sequence specificity between enzyme and substrates.

Chapter 5 reveals a RNA-cleaving DNAzyme that can ligate cleaved RNA substrates when the reaction mixture is frozen. The significance behind this chapter is that previous ligating DNAzymes require high-energy triphosphates and instead uses a 2’3’-cyclic phosphate. This 2’3’-cyclic phosphate is already a product of the cleavage reaction of the DNAzyme and the cleavage/ligation reaction is in effect recycling the same materials.

CHAPTER 1

INTRODUCTION

Francis Crick's 1970 “Central Dogma of Molecular Biology” lists three important players: DNA, RNA, and protein. This concept of how sequential information was stored and then transferred was first introduced in 1958 and has since been changed with new discoveries on the functions of each of these three key players. Many scientists have pondered the question, which of these three is the best candidate for being the first biomolecule with the ability for self-replication? DNA has long been known as the main information storage molecule, while RNA acts as the intermediate between DNA and protein, or in some cases as the template back to DNA. Protein, despite its essential roles in structure and catalysis, appears to be an informational dead-end (Figure 1.1).

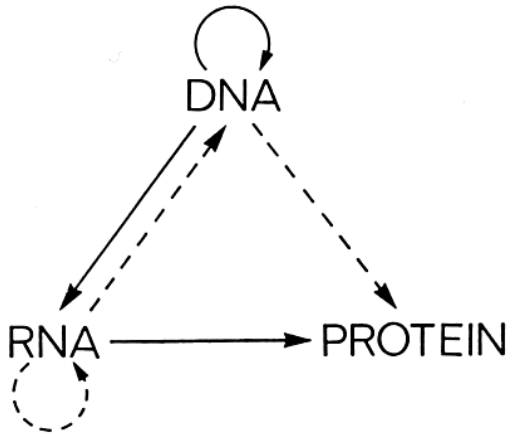

Figure 1.1: The Central Dogma as was known in 1970, with solid lines indicating probable transfers and dashed lines as possible transfers (Reprinted from Crick 1970).

RNA World Hypothesis

The "RNA World" hypothesis began in the 1960's with several authors supporting nucleic acids, not proteins, as the crucial components in a self-replicating system (Woese 1967, Orgel 1968 and Crick 1968). Watson-Crick base pairing of mononucleotides on a template strand may be sufficient in generating a complementary copy as demonstrated as early as 1968 by Sulston et al who created oligoadenylates from monomers. In contrast, the closest example of protein "replication" is from the discovery of prion proteins which only bestows secondary and tertiary information but not the peptide sequence (Prusiner 1982, Lee et al. 1996). In 1968, Crick suggested that ribosomal RNA and transfer RNA were remnants of an all RNA ancient machinery for protein synthesis. At that time, Crick stated that the protein portion of the ribosome may have replaced the primitive rRNA in the peptidyl transferase center. Today, with structure data from many bacterial ribosomes, there is much evidence that none of the ribosomal proteins are responsible for peptidyl transferase activity (Yusupov 2001), and that this activity appears to require a small portion of the ribosome's 23S rRNA.

Potential Role of Fe^{2+} in RNA catalysis

The modern ribosome requires Mg^{2+} cations for proper RNA folding and catalysis. These cations interact with the RNA phosphate groups that normally repel each other and bring them closer together. Billions of years ago, before the biologically-induced Great Oxidation Event, there was a higher concentration of dissolved Fe^{2+} in water, unlike today when almost all Fe^{2+} is rapidly oxidized into the insoluble Fe^{3+} (Anbar 2008). Fe^{2+} in the presence of oxygen may lead to a harmful environment for

RNA when hydroxyl radicals are produced in a Fenton reaction (Prousek 2007), but in the absence of oxygen, Fe^{2+} may be able to substitute for Mg^{2+} in its interaction with RNA. Quantum Mechanical calculations have shown that RNA-Mg^{2+} interactions are similar to RNA-Fe^{2+} (Figure 1.2) (Athavale et al. 2012). These cations may have been interchangeable before the atmosphere was heavily oxygenated.

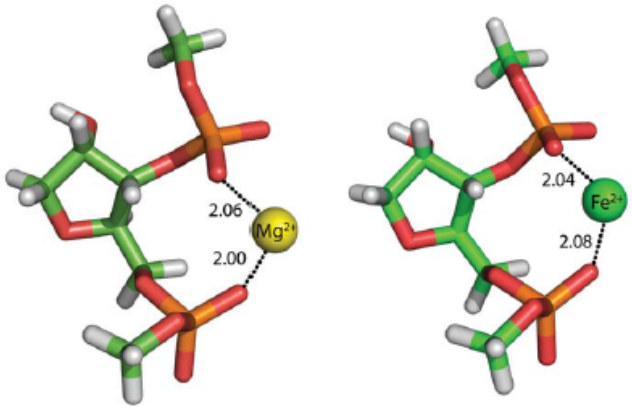

Figure 1.2: QM models for RNA-Mg^{2+} and RNA-Fe^{2+} clamps. Each cation (green and yellow spheres) is interacting with phosphate oxygen atoms (red) (Adapted from Athavale 2012).

Ribozymes Perform a Variety of Functions

In the late 1980's, the identification of the first observed ribozymes Ribonuclease P (Guerrier-Takada 1984) and self-splicing RNA (Kruger 1982) provided further support for the RNA World hypothesis; it provided evidence that RNA, without the aid of proteins, can catalyze reactions. Other natural ribozymes include the hammerhead ribozyme that can cleave and ligate (Prody et al. 1986, Hutchins et al. 1986), the hairpin ribozyme which is also able to cleave and ligate (Hampel and Tritz 1989, Felstein et al. 1989, Kazakov et al. 2006), self-splicing Group I introns (Cech 1990), and the *glmS* ribozyme that can both catalyze the production of glucosamine-6-phosphate and self-

cleavage (Winkler et al. 2004). Artificial ribozymes were also discovered in *in vitro* selection experiments, like the L1 ligase that catalyzes the formation of a 3'-5' phosphodiester bond (Robertson et al. 2001) and the R18 polymerase (Attwater et al. 2010).

Challenges to the RNA World Hypothesis

One major caveat to the RNA World hypothesis is the general instability of RNA, as opposed to DNA's long standing reputation as a stable molecule fairly resistant to degradation. RNA can be easily cleaved by hydrolysis, posing a challenge to the survival of long and complex RNA strands (Pace et al. 1991). One solution to RNA instability is the lowering of temperature, specifically temperatures which promote a eutectic mixture of solid ice and interstitial fluid composed of the remaining liquid water and solutes (Figure 1.3). It is important that temperatures cannot be too low that solutes become embedded in the ice crystal lattice or salts become too concentrated to form precipitates. Although early Earth is commonly theorized to be warm, it may have been cool enough to support freezing (Fishbaugh et al. 2007, Bada 2004).

Non-enzymatic RNA cleavage is reduced at lower temperatures (Li and Breaker 1999) and many other reactions are possible at temperatures below freezing, including the formation of precursors of purines from hydrogen cyanide (Sanchez et al. 1966), formation of dinucleotides from adenosine 2'3'-cyclic phosphate on a poly(U) template (Renz et al. 1971), ligation of short uridine oligomers (Sawai and Wada 2000) and metastable RNA dimer formation in ice (Sun et al. 2007).

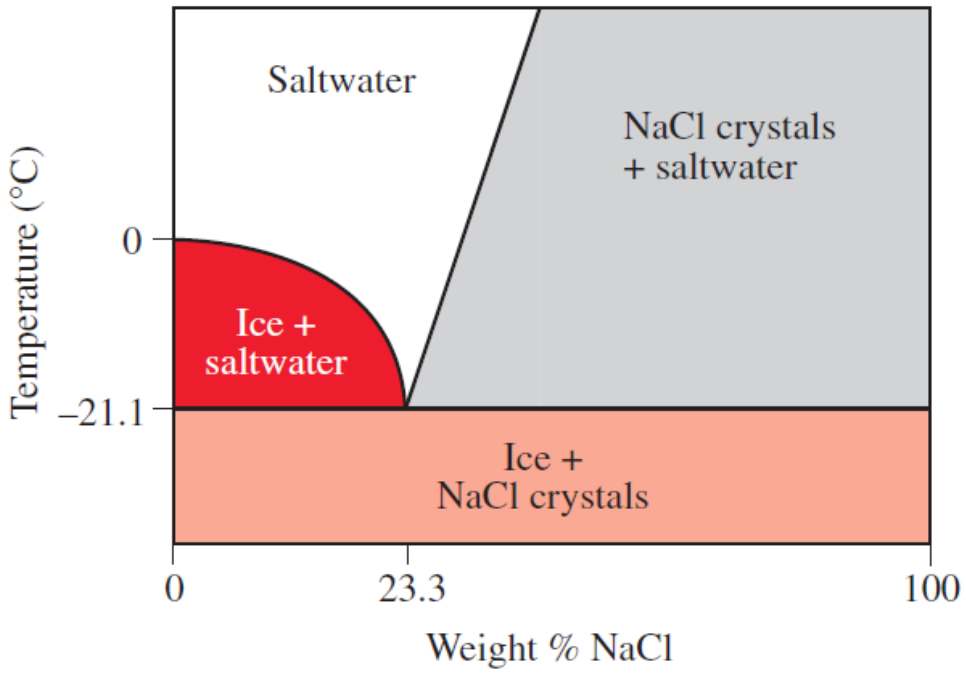

Figure 1.3: Phase diagram of NaCl with variable temperature and salt concentration. The eutectic phase exists within the triangular space labeled "ice + saltwater." Exiting the boundaries of this space will eliminate the eutectic phase (Reprinted from Clark 2003).

Another challenge of a prebiotic environment is that any existing catalytic RNAs and many important ions may be too low in concentration for function. Estimated ancient ocean concentrations of Na^+, K^+, Ca^{2+}, and Mg^{2+}, Mn^{2+}, and Zn^{2+} are >0.4, ~0.01, ~0.01, ~0.01, ~10^{-7}, and less than 10^{-12} M respectively (Mulkidjanian et al. 2012). The eutectic system of solid and liquid phases allow a concentrating effect and a lower-energy, protective environment. There is a range of temperatures for each solution that will maintain the eutectic phase; below this range the solution is solid ice with possible precipitates and above this range, the solution will be thawed back into liquid (Figure 1.3). This range is dictated by the type and concentration of solutes in the solution. The eutectic system form channels in the ice and how they network with each other determine the diffusion rate in the ice (Figure 1.4). This environment has been suggested as a

protective environment which provides some isolation of the solutes from the majority of water, inhibiting the diffusion of substrates of catalytic reactions (Trinks et al. 2005).

Dilute concentrations of RNA may be a hindrance in liquid samples, but is not the case once a solution is frozen. A notable example is the Round 18 ribozyme in Figure 1.5, an artificial RNA polymerase ribozyme that demonstrates high-fidelity template-directed RNA replication. It, however, requires mM concentrations of $MgCl_2$ and ribonucleotide triphosphates for polymerization. These high concentration requirements may have been an obstacle in liquid phase, but not in ice. Diluting the magnesium ion and nucleotide concentrations up to 200-fold does not eliminate polymerase activity (Attwater 2010).

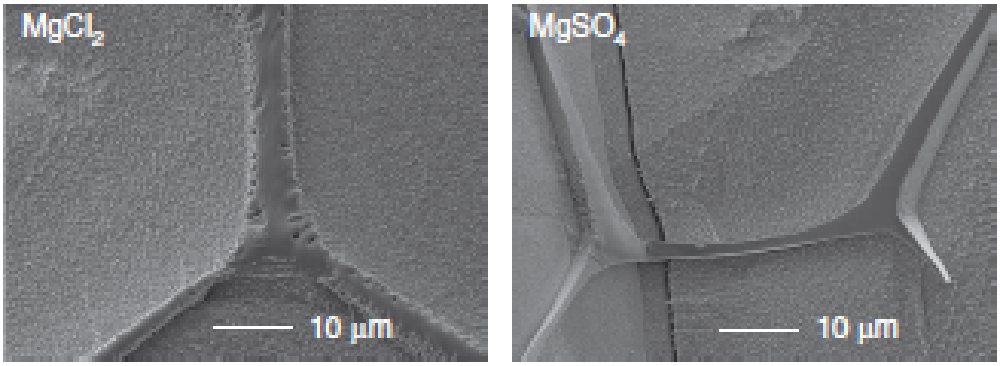

Figure 1.4: Electron Microscopy images of ice surrounding channels containing the eutectic phase. Different anions and concentration determine the ice structure in the micrometer range (Reprinted from Attwater 2010).

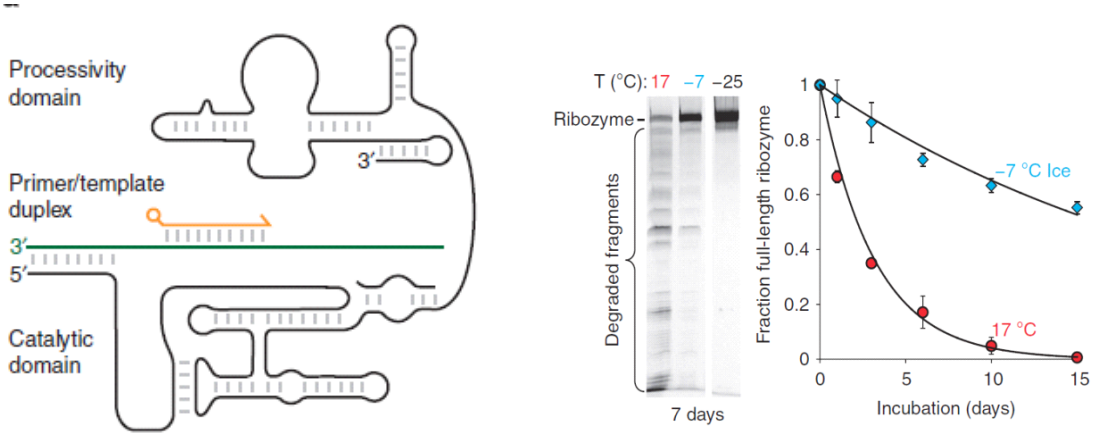

Figure 1.5: Left panel: Simplified model of Round 18 ligase with Primer in orange and Template in green. Right panel: Protection of full length ribozyme in ice. The lower the temperature the more the ribozyme is preserved over a time frame of 15 days (Adapted from Attwater 2010).

Another boon of cold incubation temperatures is the natural defense from random degradation. The Round 18 polymerase degrades completely within 15 days in 17° C, but 60% of the ribozyme retains its full length if incubated at -7°C (Figure 1.5). Longer length products from this replicase are also available at -7°C and even more extended products if the solution is frozen versus supercooled (Attwater 2010).

Ice also provides an indirect benefit to catalytic RNAs; it may help lower the breakdown of certain catalysts such as carbodiimide, a common reagent for ligation of nucleic acids. Carbodiimide-activated ligation occurs over several days in freezing temperatures when compared to room temperature or 37 °C incubation. The carbodiimide is generally longer lived the lower the temperature (data not shown).

Freezing temperatures contribute to greater stability in RNA complexes or may induce alternative conformations not easily accessible at higher temperatures. Kazakov et al in 2004 showed that truncated and divided forms of the hairpin ribozyme are still able to ligate substrates (up to 23%) in -10°C but almost no detectable activity in 37° C (Figure 1.6). Furthermore, experiments with a 21 nt RNA hairpin indicates it can form a

metastable dimer when frozen, but stays as a hairpin if incubated in temperatures above freezing (Sun et al. 2007).

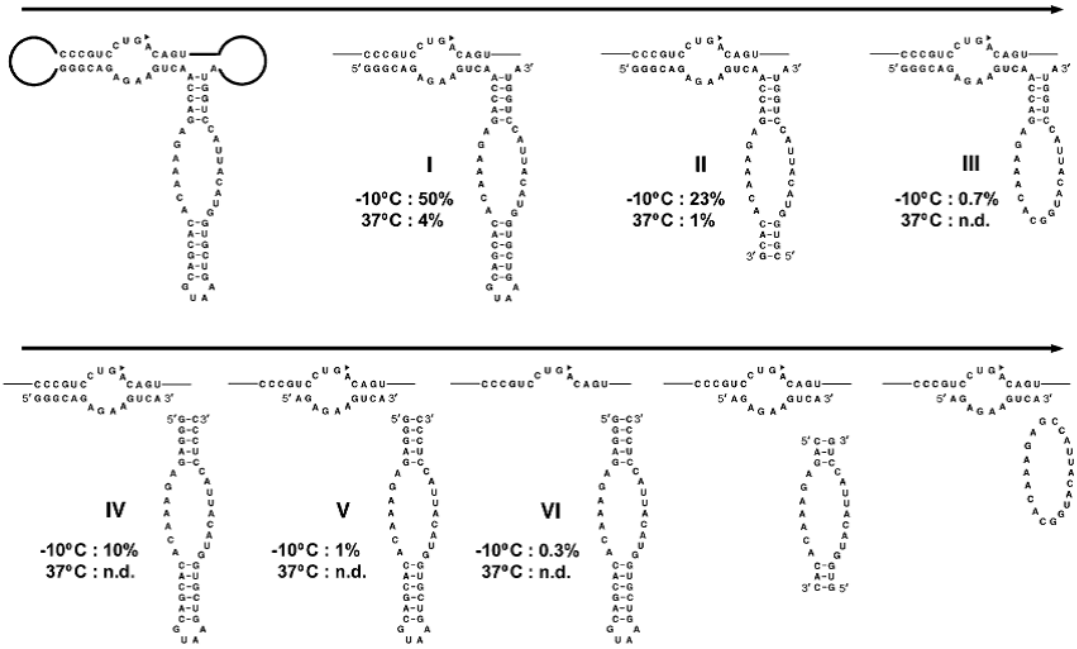

Figure 1.6: Truncated forms of the hairpin ribozyme. Indicated values represent the amount of ligated products incubated at the designated temperatures. The mutations decrease ligation activity at 37°C and in some cases it cannot be detected. Ligation yield is higher at -10°C (Reprinted from Vlassov 2005).

Hammerhead Ribozyme

The magnesium-dependent hammerhead ribozyme (HHR) is an RNA motif generally recognized as a cleaver of RNA substrates since the 1980s and has been studied extensively. However any cleavage reaction is potentially reversible. The ligation rate of a truncated hammerhead ($k_{ligation}$ = .008 min^{-1}) is about 100-fold slower than the cleavage rate (Fedor and Uhlenbeck 1992) and extending the Stems to allow loop-loop interactions show a 1300-fold higher ligation rate than the minimal hammerhead (Nelson et al. 2005). Stage-Zimmermann's version of the hammerhead (HHα1) is able to ligate better at low

temperatures, especially with the aid of a disulfide crosslinker which binds Stems I and II together (Figure 1.7). This indicates that tertiary interactions between the two stems are crucial to tipping the hammerhead enzyme from a cleavage reaction to a ligating one. Several years later, a slightly larger hammerhead, called Schist26, with extended Stems I and II demonstrated reversible cleavage-ligation reaction which boasts a 23% ligation yield with a $k_{ligation}$ of 26 min^{-1} at room temperature with no artificial linker (Figure 1.8) (Canny et al 2007). The ligation rate of this hammerhead is about 3000-fold higher than the minimal hammerhead. The Schist26 hammerhead may perform better if the incubation temperatures are dropped to below freezing, possibly promoting more stable interactions between the two stems.

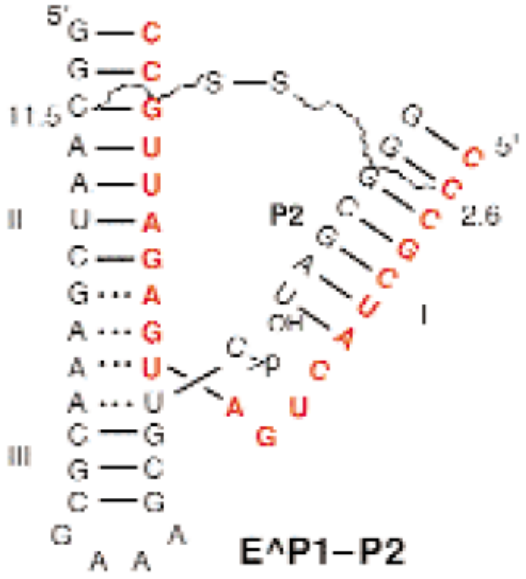

Figure 1.7: Disulfide crosslinker between Stems I and II increase HHα1 hammerhead ligation activity (Adapted from Stage-Zimmerman and Uhlenbeck 2001).

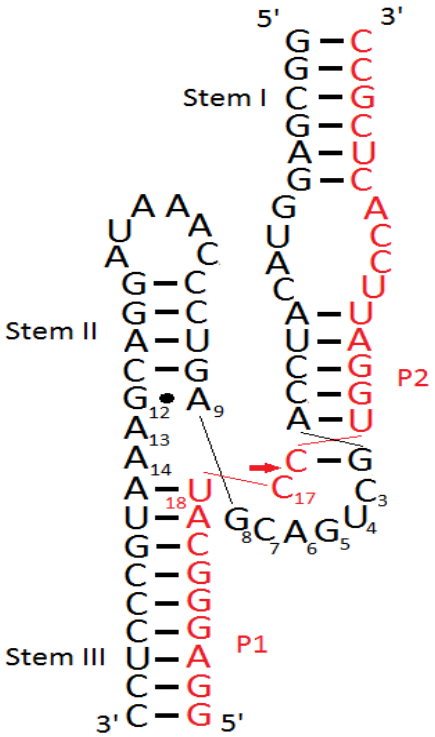

Figure 1.8: Secondary structure model of the hammerhead ribozyme from *Schistosoma mansoni* (Schist26) adapted from Pardi et al 2007. Ribozyme strand is outlined in black while the substrate is colored red. Single straight arrow between two cytosines points to the cleavage and ligation site of the full length substrate (S) which produces a 5' hydroxyl on P2 and 2'-3' cyclic phosphate on P1.

DNAzymes in the RNA World

RNA is not the only nucleic acid with catalytic activity; if an "RNA World" did exist, it may not be an "RNA [only] World." Despite the absence of naturally occurring DNAzymes, artificial ones have been in-vitro selected for RNA cleavage (Breaker and Joyce 1994, Santoro and Joyce 1997, Flynn-Charlebois 2003), as a biosensor for lead ions (Li and Lu 2000), repair enzyme for thymine dimers in DNA (Daniel and Dipankar 2004), and even as a nanomaterial for use in nanowires, nanoarchitectures and computing (Ito and Fukusaki 2004). Like the hairpin and hammerhead ribozyme, the first

discovered Dnazymes bind to complementary regions of a target RNA and cleave them in specific areas (Figure 1.9). These cleaving DNAzymes have shown efficient activity, a reported cleavage rate of ~0.01 min^{-1} for the 10-23 motif under simulated physiological conditions. DNAzyme cleavage produces two RNA fragments: a 5' hydroxyl on one and a 2',3' -cyclic phosphate, 2' or 3' phosphate on the other (Santoro and Joyce 1997). These RNA products are similar if not the same to the ones for the hairpin and hammerhead ribozymes and this may indicate that the ligation of two RNAs may occur at a reasonable rate by changing the temperature.

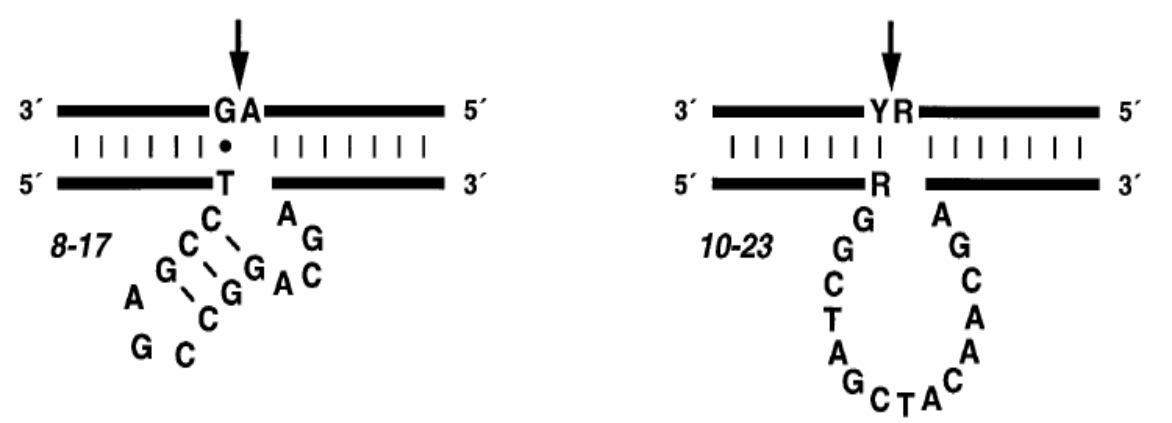

Figure 1.9: Secondary structure model of 8-17 and 10-23 dnazyme catalytic cores and binding arms. Arrows point to cleavage site in between sequence requirements of RNA substrate for successful catalysis (Reprinted from Santoro and Joyce 1997).

Summary of Thesis

The following chapters will focus on different questions about the RNA World Hypothesis. The first set of studies centers on the effect of Fe^{2+} in hammerhead ribozyme catalysis, both positive and negative impacts. This truncated ribozyme derived from a natural hammerhead motif is capable of cleaving and ligating short RNA oligos, a

fundamental activity for constructing more complex RNAs. Chapter 3 and 4 examines the catalytic activities of the hammerhead ribozyme under plausible prebiotic conditions, specifically in frozen solution. The work demonstrates that hammerhead ribozyme ligation in ice can increase the overall product yield, the complexity and diversity of the RNA products. More importantly, this freeze-induced ligation does not require the presence of divalent metal cations. The last set of studies is on RNA ligation by RNA cleaving DNAzymes, DNA sequences with catalytic activity. Like the hammerhead, freezing of the DNAzyme with cleaved substrates increases ligation rates. The addition of DNAzymes should enrich the RNA World hypothesis and show that RNA does not stand alone as a catalytic molecule with information storage.

CHAPTER 2

EFFECT OF FE^{2+} ON HAMMHERHEAD CATALYSIS

Some figures in this chapter, both in Introduction and Results sections, are reprinted from Athavale et al. 2012. The figures that appear in the Introduction belong to other co-authors, while Figure 2.6 represents the experimental data acquired by the thesis's author.

Introduction

The oldest direct evidence of life comes from fossilized stromatolites, sedimentary structures produced by mat-building communities of mostly photoautotrophic prokaryotes dated to ~3.5 billion years ago (Schopf 2006). About one billion years later, the O_2 content in the atmosphere increased (Holland 2006) and coincided with the highest known amount of banded iron formation (BIF) in geologic history (Klein 2005). Due to this Great Oxidation Event, ancient earth went from an anoxic environment with soluble Fe^{2+} to one where the excess oxygen would precipitate the iron into the BIF.

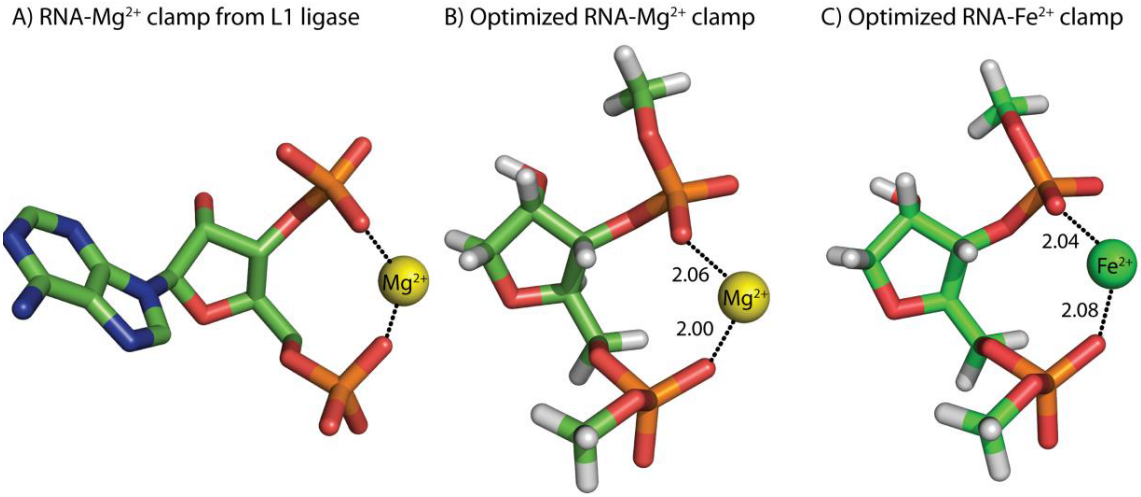

Figure 2.1: Similar conformations between the RNA-Mg^{2+} and RNA-Fe^{2+} clamps based on QM calculations (Reprinted from Athavale et al. 2012).

If the RNA World Hypothesis is true, it should predate the Great Oxidation Event, indicating that in an anoxic environment, RNAs may have been able to utilize Fe^{2+} in folding and catalysis, similar to the Mg^{2+}-RNA interactions observed today. Mg^{2+} is redox inactive and, unlike Fe^{2+} in the presence of oxygen, does not lead to the cleavage of RNA due to the generation of highly reactive radicals from Fenton chemistry. Quantum mechanical (QM) calculations for the RNA-Mg^{2+} clamp in the L1 ribozyme ligase show nearly identical RNA conformations when the Mg^{2+} is replaced with Fe^{2+} (Figure 2.1), but there are subtle differences between the two. Interactions with Fe^{2+} appear more stable and show a more negative charge is transferred from phosphate to Fe^{2+} than to Mg^{2+} by 0.14 e-. Fe^{2+} may be better in activating the phosphorous in the phosphate groups of RNA to nucleophilic attack and may favorably impact ribozyme catalysis (Athavale et al. 2012).

Selective 2'-hydroxyl acylation analyzed by primer extension (SHAPE) provides single-nucleotide resolution of secondary and tertiary structural information. SHAPE data of 2.5 mM Mg^{2+} and 2.5 mM Fe^{2+} on the P4-P6 domain of the *Tetrahymena thermophila* Group I intron show very similar reactivity profiles, supporting the theoretical claim made by QM calculations that proper folding of RNA can be achieved by either cation (Figure 2.2) (Athavale et al. 2012). Evidence of proper folding of the RNA with Fe^{2+} imply that RNA catalysis should be possible. This combined with QM predictions should show enhanced ribozyme activity.

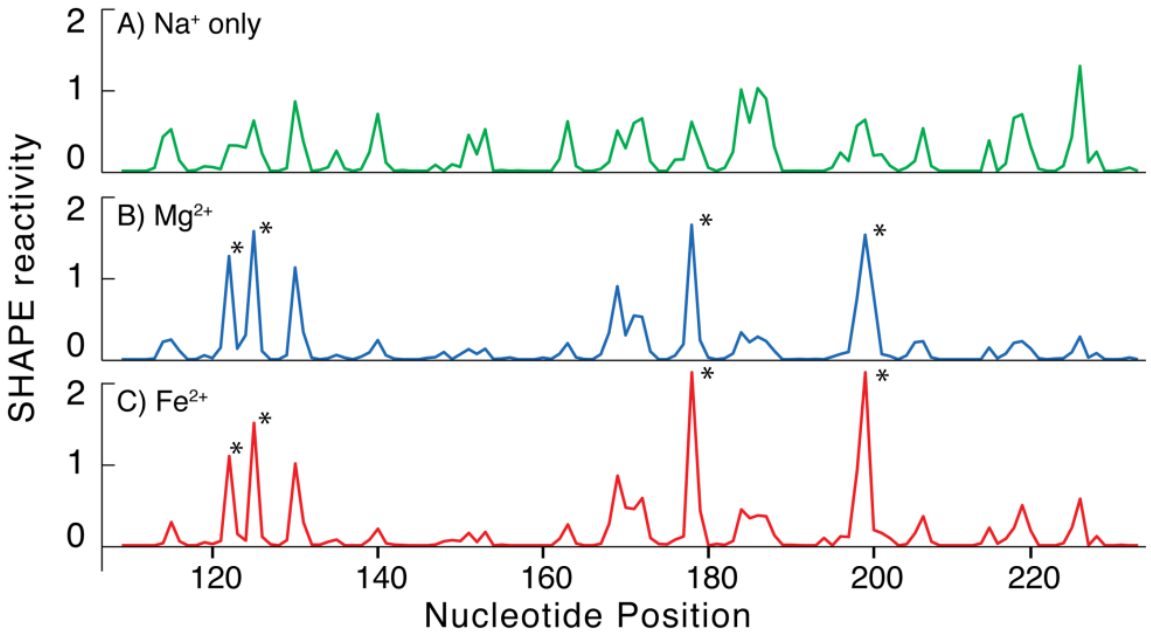

Figure 2.2: SHAPE footprinting of the P4-P6 domain of the Tetrahymena thermophila Group I intron. SHAPE profiles of the RNA with Na^{+} only as control (green), Mg^{2+} in blue, and finally Fe^{2+}in red. Mg^{2+} and Fe^{2+} show nearly identical profiles, indicating that using either cation can properly fold the P4-P6 RNA (Reprinted from Athavale 2012).

To test these predictions, the ligation activity of the Mg^{2+}-dependent L1 ligase was monitored with both Mg^{2+} and Fe^{2+}. The L1 ligase is a ribozyme selected from a random sequence population that forms into a three-helical junction and catalyzes the formation of a 3'-5' phosphodiester bond between the 3' hydroxyl group of an RNA substrate and the 5'-triphosphate end of the L1 ligase (Robertson et al. 2001). There is a 25-fold difference between the initial rate of ligation for 100 µM Mg^{2+} (1.4×10^{-6} min^{-1}) and for 100 µM Fe^{2+} (3.5 x 10-5 min^{-1}) (Figure 2.3). The enhanced ligation rate of the L1 ligase agrees with the QM prediction that Fe^{2+} would be better than Mg^{2+}.

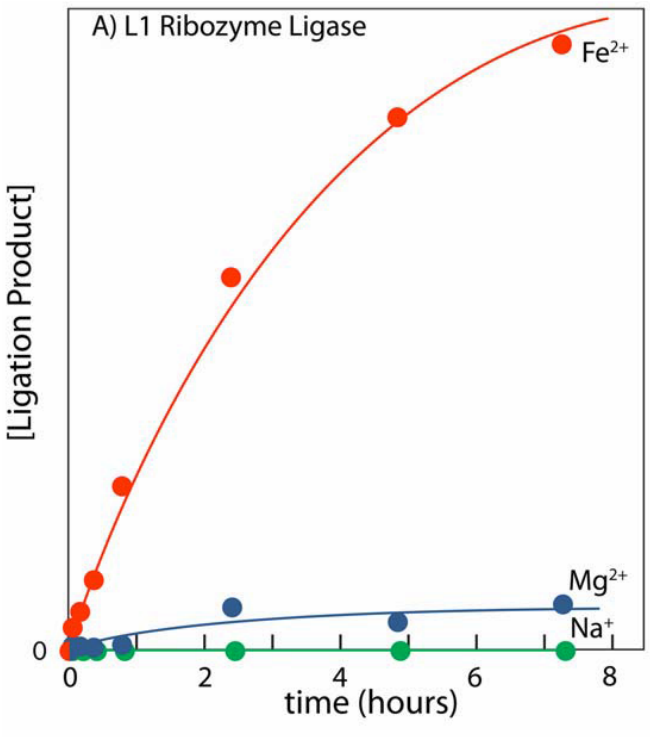

Figure 2.3: Fe^{2+} induced ligation of the L1 ligase shows a 25-fold higher initial rate of ligation than with Mg^{2+} (Reprinted from Athavale 2012).

The L1 ligase is an artificial ribozyme that requires a 5'-triphosphate for ligation. This triphosphate requirement presents a problem for the RNA World since there is no known efficient prebiotic synthesis of high-energy polyphosphates (Miller and Keefe 1995). The hammerhead ribozyme, on the other hand, can cleave a substrate in a reversible reaction, meaning that it can produce two RNA cleavage products and ligate them back together. The cleavage reaction generates a 5'-OH on the P1 fragment and a 2'3' -cyclic phosphate on P2 (Figure 2.4), which are not uncommon products. In fact the hairpin, HDV, VS, and *glmS* ribozymes also produce a 5' hydroxyl and cyclic phosphate (Ferre-D'amare and Scott 2010).

The ribozyme employs several strategies for efficient activity: general acid/base chemistry to deprotonate the 2' OH and protonation of the 5' oxygen, neutralization of phosphate backbone for complex stability, and geometric alignment for in-line

nucleophilic attack by the 2'O (Emilsson et al. 2003). The extensively studied hammerhead RNA enzyme utilizes a variety of divalent metal cations for cleavage. The divalent cation not only coordinates the phosphates of the RNA for proper folding, but may also be indirectly involved in general acid/base chemistry of the reaction by interacting with one of the oxygens on the scissile phosphate (Ward and Derose 2012). This interaction makes the phosphorous more electrophilic and more likely for nucleophilic attack by the 2' oxygen (Figure 2.5). According to the QM calculations for RNA-Fe^{2+} interactions, replacing Mg^{2+} with Fe^{2+} should better activate the scissile phosphate and perhaps enhance ribozyme activity.

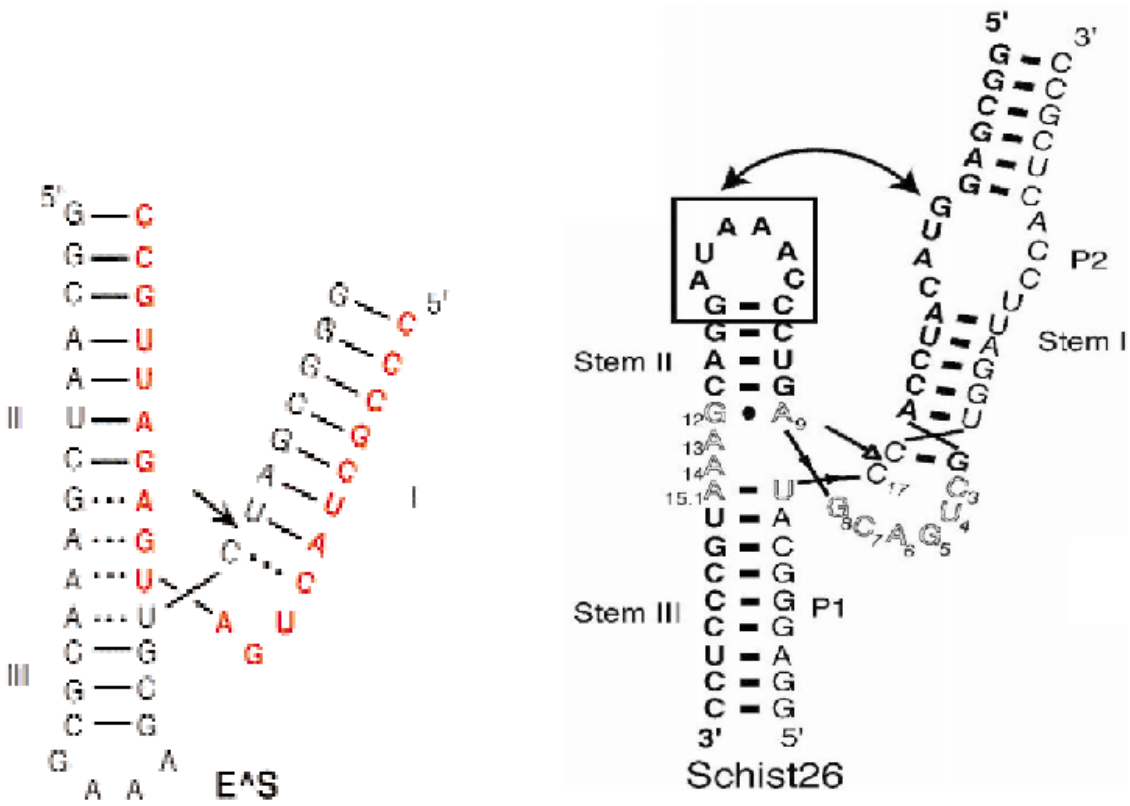

Figure 2.4: Secondary structure of truncated HHα1 hammerhead (Adapted from Stage-Zimmerman and Uhlenbeck 2001) and Schist26 hammerhead (Adapted from Canny et al. 2007). The truncated hammerhead enzyme strand is in red while the substrate is in black. The Schist26 hammerhead has longer stems and is able to ligate better than the truncated version due to the tertiary interactions of the loops between Stems I and II. The arrows indicate the cleavage/ligation site.

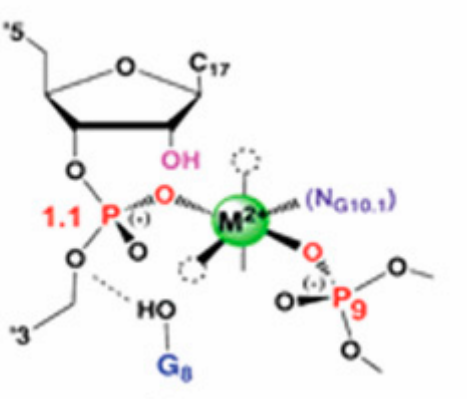

Figure 2.5: Mn^{2+} coordination of the scissile phosphate in the active site. The divalent metal cation (green) interacts with the oxygen from the scissile phosphate 1.1 (red), resulting in a more electrophilic phosphorous for the nucleophilic 2' oxygen (pink) to attack (Reprinted from Ward and DeRose 2012).

Materials and Methods

Hammerhead Cleavage Reaction

All manipulations of the hammerhead RNA in the presence of Fe2+ were carried out in a Coy chamber with an atmosphere of 85% N2, 10% CO2, 5% H2. The hammerhead ribozyme-substrate was based on the unmodified HHα1 RNA (Stage-Zimmerman and Uhlenbeck 2001). A 31 nucleotide substrate strand (5' GGCAAUCGAAACGCGAAAGCGUCUAGCGGGC- 3'), labeled at the 3'- end with FAM, and the 21 nucleotide ribozyme strand (5'- CCCGCUACUGAUGAGAUUGCC-3') were purchased from IDT. Substrate and ribozyme strands (typical molar ratio used was 1:1000) were lyophilized separately, transferred to the anaerobic chamber, left open for several hours, and resuspended in 50 mM HEPES, pH 7.5 (pH adjusted with KOH). The buffer had previously been deoxygenated by bubbling with argon for several hours. The strands were annealed inside the anaerobic chamber by incubating at 90 °C for 2 min and cooling to room temperature over 30 min. Reactions (150 µL final volume) were initiated by addition of 1.5 µL of cation solution (Fe^{2+} or Mg^{2+}). At predetermined time points, 20

μL aliquots were withdrawn and quenched by treatment with divalent cation chelating beads. The beads and the associated divalent cations were removed with a spin column, and the samples were frozen and stored at -80 °C. For gel analysis, 1 μL of reaction mixture was mixed with 9 μL loading buffer (8 M urea, 16 TTE, 10% glycerol) and denatured by heating to 90 °C for 2 minutes. The intact 31 nucleotide substrate and 7 nucleotide product were separated by capillary electrophoresis and quantified as described (Athavale et al. 2012). Controls were performed to ensure that oxygen had no effect on Mg^{2+}-induced reactions (Shreyas Athavale, unpublished).

Hammerhead Ligation Reaction

The Schist26 hammerhead ribozyme was chosen for ligation experiments due to its higher ligation rate. The 49-nt Schist26 ribozyme strand (E) was generated by in vitro transcription of a 68 bp DNA containing the template sequence joined to a T7 promoter. The DNA template strands (Integrated DNA Technologies, Coralville, Iowa, USA) were characterized by denaturing gel electrophoresis to verify purity. They were heated to 90 ^{0}C for two min and slowly cooled to form a duplex before being transcribed with an Ambion MEGAscript T7 kit (Life Technologies, Grand Island, New York, USA). The resulting RNA was gel purified. The ligated RNA product P1•P2: 5'GGAGGGCAUCCUGGAUUCCACUCGCC3' was chemically synthesized (Integrated DNA Technologies), characterized by denaturing gel electrophoresis and modified if necessary as described below.

The P1>p strand, which is the P1 sequence with a 2'3' -cyclic phosphate at its 3' end, was generated from Schist26 -facilitated cleavage of P1•P2. When P1•P2 was cleaved by the hammerhead to obtain P1>p, it was first 5' 32P-end labeled using T4 polynucleotide kinase (3'phosphatase minus) and ^{32}P-γATP. 10 pmoles of P1•P2 was typically prepared in a 50 μL reaction. 100 pmoles of the E strand was added to 5' end-labeled P1•P2 in kinase buffer, and the reaction was cycled four times for 2 min at 70 ^{0}C and 20 min at

25 °C. P1>p was purified from its unmodified substrates by 20% denaturing PAGE, excised, and ethanol precipitated with glycogen.

All manipulations of this hammerhead RNA in the presence of Fe^{2+} were carried out in a Coy chamber with the same atmosphere listed above. A typical master mix contained 0.5 μM ribozyme strand, 2.5 μM P2 fragment, and trace amounts of ^{32}P-labeled P1>p in a 100 μL solution of 50 mM PIPES pH 8.0, 100 mM NaCl, and 0.1 mM EDTA (NTE buffer). Sodium mesh chelating resin (Sigma) was used to remove trace amounts of Mg^{2+} in buffers and reaction mixtures. The buffer had previously been deoxygenated by bubbling with argon for several hours. The chelating resin was included in the RNA annealing step in which the reaction mixture was heated to 80 °C for 2 min and then allowed to cool at 25 °C for 30 min. The resin was removed by filter centrifugation. Ligation reactions in solution at 25 °C were initiated by adding $FeCl_2$ to the master mix to give a final concentration of 1 mM. Reactions were halted by adding a stopping solution of 80% deionized formamide and 20 mM EDTA with bromophenol blue and xylene cyanol in a 4:1 volume ratio to the sample. Products were run on a 12% denaturing polyacrylamide gel (7 M urea) and analyzed with a GE Typhoon Imager and Fuji Multi Gauge Imaging software.

Results

Cleavage activity of HHα1 hammerhead is enhanced with Fe^{2+}

In these reactions the initial rate of hammerhead cleavage in 25 μM Mg^{2+} is 0.011 min^{-1}, while the initial rate of cleavage in 25 μM Fe^{2+} is 0.035 min^{-1}, which is 3-fold higher (Figure 2.6). The maximum fraction of cleaved substrate was about 3-fold greater in Fe^{2+} versus Mg^{2+}. When 100 μM of these two divalent cations were employed, Fe^{2+} again showed a higher initial rate of cleavage of ~3.5 fold. The enhanced cleavage reaction of the hammerhead shows that Fe^{2+} is a better metal cofactor than Mg^{2+}.

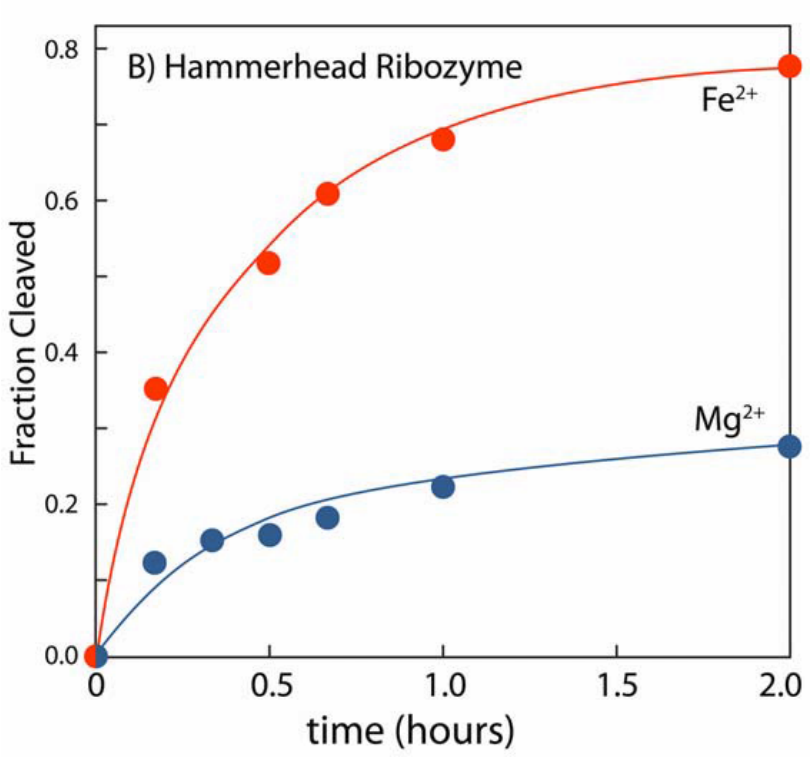

Figure 2.6: Hammerhead ribozyme activity is enhanced in Fe^{2+} compared to Mg^{2+}. Cleavage reactions were initiated by addition of $FeCl_2$ or $MgCl_2$ from stock solutions to a final concentration of 25 μM (Reprinted from Athavale et al. 2012).

Ligation activity of the Schist26 hammerhead with Fe2+

Ligation experiments were done with the Schist26 hammerhead ribozyme because it ligates better than the minimal HHα1 ribozyme ($k_{ligation}$ = 0.008 min^{-1} and $k_{ligation}$ = 26 min^{-1} respectively) (Stage-Zimmerman and Uhlenbeck 2001, Canny et al. 2007). According to Canny et al, when 1 mM $MgCl_2$ was added to induce ligation, their yield reached a maximum of 6% in about 5 minutes, k_{ligate} of ~1.5. With Fe^{2+} present, the reaction is faster and shows a higher maximum yield of 10% by the first time point at 20 seconds (Figure 2.7). An accurate k_{ligate} is difficult to obtain due to the high ligation rate and is further complicated by the aggregation of the radiolabeled P1>P RNA. The ligation yield also appears to decline with time, a similar pattern as seen with Mg^{2+} (Roy 2008). Whether this is due to the breaking of the cyclic phosphate of the P1>P RNA,

resulting in an irreversible cleavage reaction of the product, or some of the P1•P2 product is being sequestered in this aggregate band is still unclear.

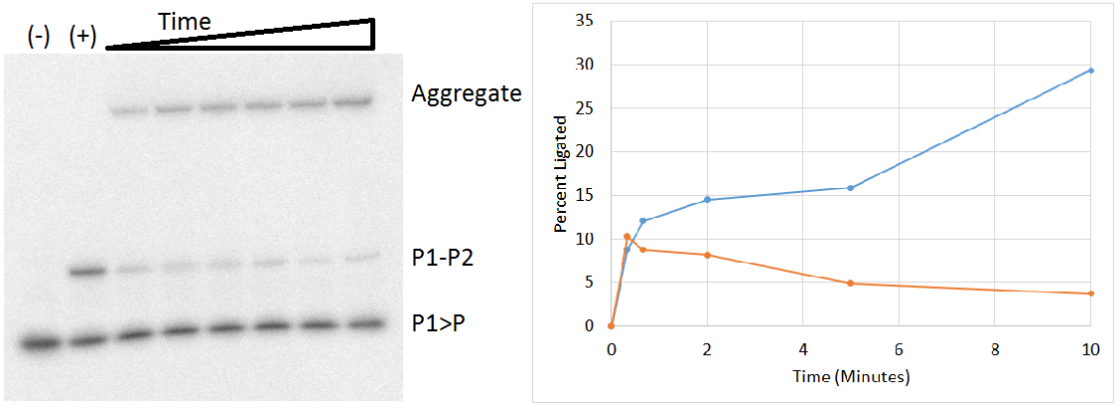

Figure 2.7: Fe^{2+}-induced ligation by the Schist26 hammerhead ribozyme at 25 °C. A) 12% PAGE separating ^{32}P-labeled P1>P from ligated product ^{32}P-labeled P1•P2 RNA and RNA aggregation. Reaction was started with the addition of 1mM $FeCl_2$ and aliquots were taken out at different time points. (-) is the negative control lane and (+) is the positive control. B) Plot of percent ligation yield (orange line) and increasing RNA aggregation (blue line).

RNA aggregation after the addition of Fe^{2+}

Aggregation of RNA in the Schist26 hammerhead ligation experiments by Fe^{2+} is visible even in the first time point at 20 seconds and increases with time (Figure 2.7). The aggregation band shows only ^{32}P-labeled P1 or ^{32}P-labeled P1•P2, trapped at the bottom of the well, unable to penetrate the gel. It is unknown if it has also captured the unlabeled hammerhead enzyme and P2. Aggregates appear more quickly if the initial concentration of Fe^{2+} introduced into the reaction mixture is more concentrated even if the final concentration of Fe^{2+} is the same; it does not eliminate RNA aggregation, only delays it. Aggregation breakup is possible to an extent and is dependent on buffer used. Tris buffer and PIPES were both used, but aggregate breakup was mostly successful when the reaction mixture containing Tris was heated in a solution of formamide and 20 mM EDTA at 90 °C for 2 minutes and then snap cooled before loading onto the gel.

Aggregates in PIPES appear to be fairly resistant to heating and formamide denaturation. Aggregation was not observed for the HHα1 cleavage experiments in HEPES buffer using μM concentrations of Fe^{2+}. This suggests that mM concentrations of Fe^{2+} and buffer choice influence the formation of hardy aggregates resistant to denaturing.

Discussion

The work on Fe^{2+} on RNA catalysis adds another aspect to the RNA World hypothesis. Before the Great Oxidation Event, Fe^{2+} may have been abundant in an anoxic early earth and may have been involved in ancient RNA folding and catalysis. QM calculations of RNA-Fe^{2+} clamps, SHAPE data of P4-P6 RNA folding similarly with both Fe^{2+} and Mg^{2+}, and enhanced ligation of RNA activity all support this (Athavale 2012).

The significance behind using the hammerhead ribozyme for Fe^{2+} studies is that it is a natural ribozyme that can reversibly cleave an RNA substrate. The cleavage products it generates are the 5'OH on one RNA fragment and a 2'3'-cyclic phosphate on the other. The HHα1 minimal hammerhead is an efficient cleaver (Stage-Zimmerman and Uhlenbeck 2001), while the Schist26 ribozyme is known to be both an efficient cleaver and ligase (Canny et al. 2007). Fe^{2+}-induced ligation and cleavage were tested.

As predicted by QM calculations, cleavage and ligation is enhanced when Fe^{2+} is used instead of Mg^{2+}. Both the cleavage rate and max yield for the HHα1 is 3-fold higher with iron than with magnesium. Ligation also shows enhanced rate and yield, although determining either of these values accurately is difficult due to RNA aggregation.

This has implications for the RNA World. If RNA were to use Fe^{2+}, not only must it utilize iron in an anoxic environment to avoid degradation but it may need to be careful

of unidentified factors that may induce the formation of RNA aggregates. Before the Great Oxidation Event, Fe^{2+} may have provided more benefits than drawbacks, but afterwards, it was too harmful and was replaced with other divalent cations.

CHAPTER 3

HAMMERHEAD RIBOZYME LIGATION IN ICE

Introduction

RNAs in modern organisms serve as catalysts in splicing and translation, as well as in information transfer and regulatory processes (Darnell 2011). The multiple functions of biological RNAs, as well as the expanding catalytic repertoire associated with RNA (Johnston et al. 2001; Turk et al. 2010; Biondi et al. 2012; Hsiao et al. 2013) lend credibility to the hypothesis that RNA served as both catalysts and self-replicating information storage at the beginning of evolution (Gilbert 1986; Joyce 1989). Although evidence supporting this premise has accumulated, the fragility of RNA in aqueous solutions has been recognized as a difficulty for the emergence of self-replicating RNA (Pace 1991; Levy and Miller 1998; Li and Breaker 1999; Bada and Lazcano 2002).

Several conditions have been proposed that may inhibit RNA degradation sufficiently to allow RNA synthesis reactions to exceed the rate of degradation. They include selective absorption onto mineral surfaces (Ferris et al. 1996), compartmentalization with lipid-like membranes (Adamala and Szostak 2013) and freezing of aqueous solutions (Kanavarioti et al. 2001; Bada and Lazcano 2002). Freezing aqueous solutions at temperatures that result in a eutectic system of crystalline ice and interstitial liquid provide several advantages (Kanavarioti et al. 2001; Vlassov et al. 2004; Vlassov et al. 2005). This environment minimizes RNA degradation, yet enables reactions that have the potential to promote the synthesis and evolution of RNA molecules.

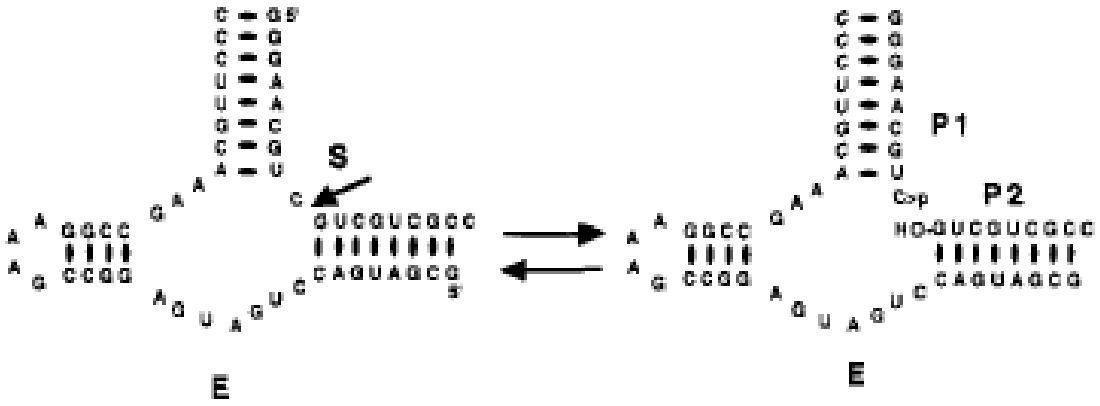

Figure 3.1. Secondary structure of minimal hammerhead. E represents the hammerhead ribozyme and S is for the substrate of the cleavage reaction. Cleavage produces a P1 with a 2'3' -cyclic phosphate and a P2 with a 5' OH (Reprinted from Hertel et al. 1994).

Reactions involving RNA that have been demonstrated in frozen solutions include: the formation of dinucleotides from adenosine 2',3' cyclic phosphate (Renz et al. 1971), synthesis of polynucleotides from imidazole-activated mononucleotides (Kanavarioti et al. 2001; Trinks et al. 2005), formation of metastable duplexes from RNA hairpins (Sun et al. 2007), and extension of RNA primers by an in vitro selected ribozyme (Attwater et al. 2010). Studies on the hairpin ribozyme (HPR) showed that freezing can induce self-ligation, as well as trans-ligation of RNA fragments in the absence of divalent cations (Kazakov et al. 1998; Vlassov et al. 2004; Kazakov et al. 2006). The HPR and several of its truncated derivatives were able to ligate RNA fragments with 5-OH and 2'3' cyclic phosphate termini to form 5'- 3' phosphodiester bonds.

In this chapter we examine the activity of the *Schistosoma mansoni* hammerhead ribozyme (Schist26). Although the hammerhead and hairpin ribozymes catalyze the same reversible cleavage-ligation reaction of a phosphodiester bond, they are structurally distinct RNAs with different biochemical properties (Fedor 2009). Unlike hairpin ribozymes, which favors ligation over cleavage under ambient conditions, the hammerhead ribozyme's cleavage rate typically dominates its ligation rate. This

ribozyme was first discovered in the satellite RNA of the tobacco ringspot virus (Hutchins et al. 1986) and in RNA transcripts of the avocado sunblotch viroid (Prody et al. 1986). Its signature characteristic was to catalyze a reaction of self-cleavage that processed RNA transcripts of multimeric genomes. The hammerhead ribozyme could also ligate together its own cleavage products (Prody et al. 1986). Since its discovery in 1986, the hammerhead motif has been shown to be pervasive in all three domains of life via bioinformatics analysis (De la Pena et al. 2003; De la Pena and Garcia-Robles 2010; Perreault et al. 2011; Hammann et al. 2012).

Studies characterizing the core sequence and structure required for this RNA's catalytic activity led to minimal sized hammerheads which were extensively studied (Forster and Symons 1987; Uhlenbeck 1987; Hertel et al. 1996; Birikh et al. 1997). The minimal construct consists of a conserved core with three helixes (Figure 3.1). Unfortunately, while this truncated version of the ribozyme eased crystallization, it was not as efficient in cleavage as its native counterpart which had longer stems to accommodate an internal and hairpin loop that formed tertiary interactions (Penedo et al. 2004).

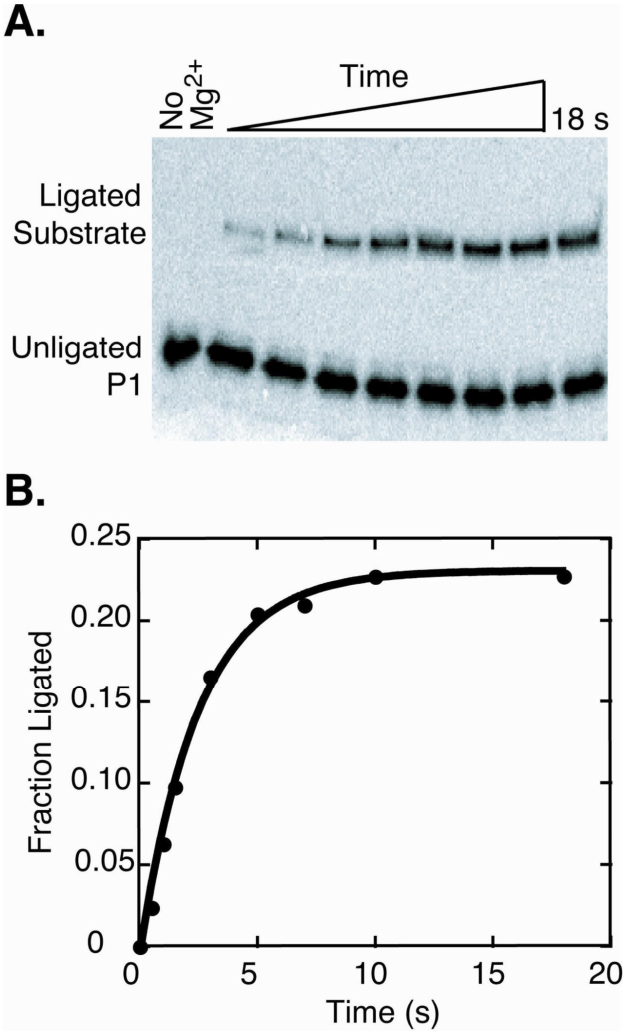

Figure 3.2. Single turnover ligation reaction over the course of 18 seconds. A) PAGE showing ^{32}P-labeled ligated substrate increasing in amount after the addition of 10mM Mg^{2+}. B) Fraction ligated reaches a maximum at 23% (Reprinted from Canny et al. 2007).

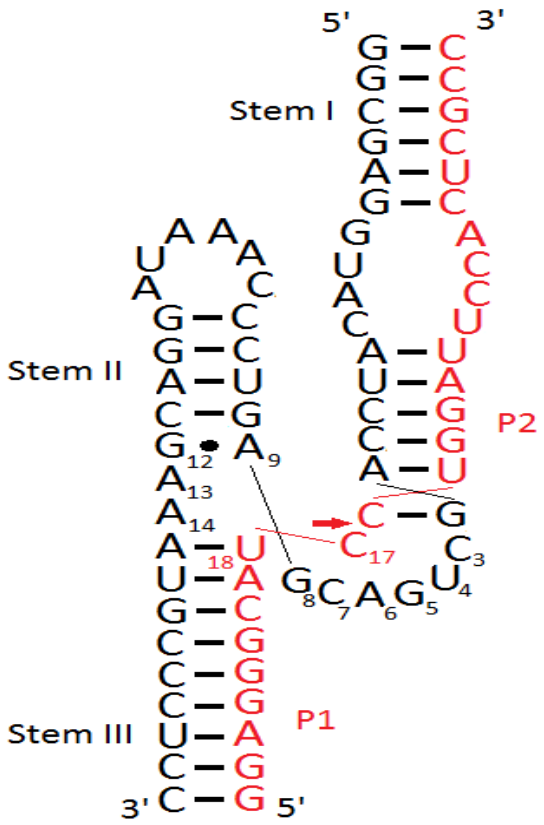

Figure 3.3: Schist26 hammerhead with labeled Stems. Substrates P1 and P2 are indicated in red. Enzyme strand is in black. Arrow points to the ligation/cleavage site (Adapted from Canny et al. 2007).

Minimal size hammerhead ribozymes exhibit efficient cleavage in 10 mM Mg^{2+} in solution, but have a very low ligation rate, producing an internal equilibrium constant of $K_{eq,int} = k_{cleave}/k_{ligate}$ ~130 (Hertel et al. 1994). A large increase in ligation rate at 25 ^{o}C was observed when Stems I and II of a minimal hammerhead (HHα10) were cross-linked with a disulfide bond (Stage-Zimmermann and Uhlenbeck 2001). Relatively efficient ligation by a natural hammerhead ribozyme was demonstrated by Canny et al in their study of the *Schistosoma mansoni* hammerhead (Figure 3.2) (Canny et al. 2007). This hammerhead has tertiary loop-loop interactions between Stems I and II that influence its activity (De la Pena et al. 2003; Khvorova et al. 2003) (Figure 3.3). In 100 mM NaCl solutions containing 0.1 mM to 10 mM Mg^{2+} *Schistosoma* hammerhead had an internal equilibrium constant of k_{cleave}/k_{ligate} in the range of 1.5 to 3 (Canny et al. 2007). Cleavage

and ligation activity were minimal or not observed in the absence of Mg^{2+} in the moderate ionic strength solution. Here we examined the catalytic activity of the *Schistosoma* hammerhead and its substrate requirements in frozen solutions. Our studies show that this ribozyme can ligate RNA oligomers in frozen solutions in the absence of divalent metal ions to a greater extent than occurs at 25 ^{o}C with Mg^{2+}. The effect on ligation of different anions, cations, pH, amino acids, and solutes that can influence water activity was examined. The nature of the anion had a significant influence on ligation in the frozen eutectic system.

Materials and Methods

RNA oligomers and modification

The 49-nt *S. mansoni* hammerhead ribozyme strand (E) was generated by in vitro transcription of a 68 bp DNA containing the template sequence joined to a T7 promoter. The DNA template strands (IDT DNA) were characterized by denaturing gel electrophoresis to verify purity. They were heated to 90 ^{0}C for two min and slowly cooled to form a duplex before being transcribed with an Ambion MEGAscript T7 kit. The resulting RNA was gel purified. Other RNA oligomers were chemically synthesized (IDT DNA), characterized by denaturing gel electrophoresis and modified if necessary as described below. They were P1-p: 5'GGAGGGCAUCp3', P2: 5'CUGGAUUCCACUCGCC3', P1•P2: 5'GGAGGGCAUCCUGGAUUCCACUCGCC3'. Figure 3.3 displays the E and P1•P2 strands assembled as the *S. mansoni* hammerhead ribozyme.

The P1>p strand, which is the P1 sequence with a 2'3' cyclic phosphate at its 3' end, was generated either from hammerhead ribozyme-facilitated cleavage of P1•P2, or by treatment of P1 with 50 mM 1-ethyl-3-[3-dimethylaminopropyl] carbodiimide (EDC) in 100mM MES pH 5.5. Cleavage of 10 pmoles of P1•P2 followed after it was 5' ^{32}P-end

labeled using T4 polynucleotide kinase (3'phosphatase minus) and ^{32}P-γATP in a 50 ul reaction. 100 pmoles of the E strand was added to 5' end-labeled P1•P2 in kinase buffer, and the reaction cycled four times for 2 min at 70 ^{0}C and 20 min at 25 ^{0}C. P1>p was purified from its unmodified substrates by 20% denaturing PAGE, excised, and ethanol precipitated with glycogen.

Ligation reactions

A typical master mix contained 0.5 µM ribozyme strand, 2.5 µM P2 fragment, and trace amounts of ^{32}P-labeled P1>p in a 100 uL solution of 50 mM Tris pH 8.0, 100 mM NaCl, and 0.1 mM EDTA (NTE buffer). Sodium mesh chelating resin (Sigma) was used to remove trace amounts of Mg^{2+} in buffers and reaction mixtures. The chelating resin was included in the RNA annealing step in which the reaction mixture was heated to 80 ^{0}C for 2 min and then allowed to cool at 25 ^{0}C for 30 min. The resin was removed by filter centrifugation. Freezing-induced ligation was initiated by freezing 10 uL aliquots in a -80 ^{0}C ethanol bath for 1 min and rapidly transferring the reaction to a temperature controlled polyethylene glycol-water bath. The quick freezing step avoided variations in the rate of freezing for timed reactions. Samples placed directly in the bath gave the same results in overnight reactions. Ligation reactions in solution at 25 ^{0}C were initiated by adding $MgCl_2$ to the master mix to give a final concentration of 5 mM. Reactions were halted by adding cold stopping solution deionized formamide and 20 mM EDTA with bromophenol blue and xylene cyanol in a 4:1 ratio to the sample. Products were run on a 12% denaturing polyacrylamide gel (7 M urea) and analyzed with a GE Typhoon Imager and Fuji Multi Gauge Imaging software.

Measurement of pH in ice

5 mL solutions of different buffers, along with cut strips of Baker-pHIX pH 4.5-10 from J.T. Baker, were placed in a 36 well plate and then frozen for 3 hours at the indicated

temperature. Pictures were taken before at room temperature and immediately after freezing before any significant thawing occurred (Figure 3.12).

Results

Ligation activity of the hammerhead ribozyme in liquid

The *trans* construct of the *Schistosoma mansoni* hammerhead ribozyme is shown in Figure 2. Single turnover kinetic experiments at 25 ^{0}C have shown that the fraction of ^{32}P-labeled P1>p ligating to P2 plateaus at ~23% within 20 seconds (Canny et al. 2007). We obtained a similar value under comparable conditions, and also observed little to no cleavage or ligation in the absence of Mg^{2+} consistent with previous studies at moderate ionic strength (Canny et al. 2004).

The ligation experiments done by Canny et al in 2004 showed a remarkably fast reaction with a $k_{obs,\ ligate}$ of ~26 min^{-1}, plateauing within 10 seconds with the full length Schist26 hammerhead ribozyme. We extended the experiment and found that the rapid increase is soon followed by a gradual decrease of the product yield (Figure 3.4). Since the reaction did not reach equilibrium, this implies that there is another reaction separate to the cleavage/ligation of P1>p and P2 to P1•P2. Substituting $MgCl_2$ for $CaCl_2$ shows a similar product yield at 20 seconds and maintains ligation products after 2 hours. Alternatively switching the Tris pH 8.0 with PIPES pH 8.0 does not prevent the decline of the amount of product but instead slows down the rate. By the end of 2 hours, using $MgCl_2$ will have reduced the max yield by over 10%, while $CaCl_2$ is about a 5% loss. This separate reaction to the cleavage/ligation appears to be especially exacerbated by the combination of $MgCl_2$ and Tris buffer. Our results are consistent with the observation by Roy indicating the 2'3' cyclic phosphate of P1>p opens with time in the presence of the Schist26 complex and high Mg^{2+} concentration, in which the dynamic ligase/cleavage reaction trends irreversibly toward the cleaved state of P1 and P2 (Roy 2008) (Figure

S3.1). An experiment was done to test whether the $MgCl_2$ can interact with only the P1>p, opening the cyclic phosphate and thereby making the P1 fragment unusable in ligation, but after incubation at 25 ^{0}C, it showed no bandshift to indicate that the P1>p had lost its cyclic phosphate (Figure 3.5).

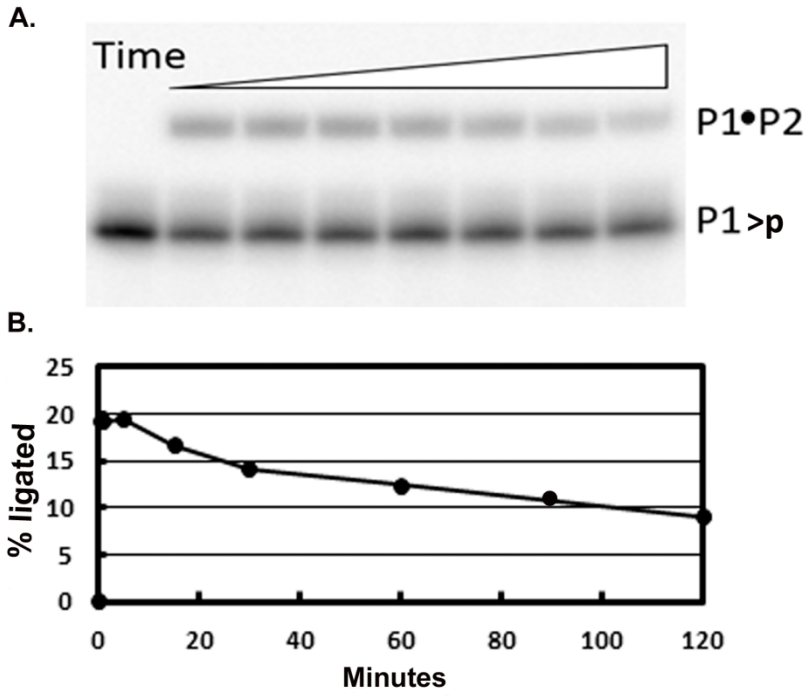

Figure 3.4. Single turnover ligation kinetics of ^{32}P-labeled P1>p and P2 oligomer catalyzed by the hammerhead ribozyme at 25 ^{0}C. A) Left lane is aliquot from reaction prior to addition of $MgCl_2$. Other lanes show aliquots removed at various times after $MgCl_2$ is added to give 5 mM Mg^{2+}. B) Plot of the percentage of P1>p ligated to P1•P2 as a function of time.

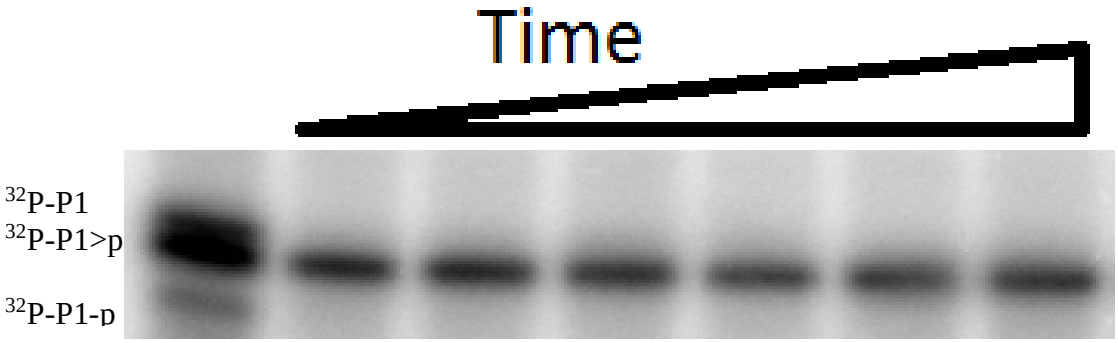

Figure 3.5: 20% PAGE of ^{32}P-P1>p in the presence of 10 mM $MgCl_2$ at room temperature. The first lane has three markers: ^{32}P-P1 (with no phosphate), ^{32}P-P1>p (2'3' -cyclic phosphate), and ^{32}P-P1-p (phosphate on the 3'). The individual lanes correspond to different time points after $MgCl_2$ was added and no bandshift is visible.

Although Mg^{2+} greatly enhances ligation in the hammerhead ribozyme, divalent cations are not an absolute requirement for ligation even at moderate ionic strength. Buffer choice and incubation temperature also influence ligation. Using NTE buffer without $MgCl_2$ can induce a small amount of ligation if the solution is supercooled to below -10 ^{0}C and incubated extended to several days. Incubating for three days gives a 2% ligation yield. If the Tris pH is changed to 7.0, this value increases to 4%. Using a different buffer such as sodium phosphate pH 8.0 gave 6% ligation yield after 24 hrs in a supercooled solution at -10 ^{0}C. The low temperature may inhibit the side reaction in which the 2'3' cyclic phosphate of P1>p is opened, and/or enhance the ratio of ligation to cleavage rates. The ligation yield without $MgCl_2$ at moderate ionic strength is still much lower than can be achieved with freezing.

Ligation activity of the hammerhead ribozyme in ice

We examined if this Schist26 hammerhead ribozyme exhibited the ability to ligate RNA in a frozen solution lacking divalent cations as previously demonstrated for the HPR (Vlassov et al. 2004). Figure 3.6A shows that the Schist26 can indeed ligate P1>p and P2 under these conditions. The percentage of P1>p ligated to P2 was 30% for

samples that were quick-frozen in NTE solvent (0.1 M NaCl, 50 mM Tris (pH 8.0), 1 mM EDTA) and incubated at -10 ^{0}C for 24 hours. Freezing-induced ligation was observed at temperatures between -7 ^{0}C and -20 ^{0}C with the maximum yield for the above solvent occurring between -10 ^{0}C and -15 ^{0}C. When a reaction tube was placed in a -10 ^{0}C freezer so that the sample remained a super-cooled liquid for 24 hours very little ligation was observed (Figure 3.6A and B). Incubating a reaction tube at -80 ^{0}C exhibited about 2% ligation.

Figure 3.6C shows the time course of a ligation reaction at -20 ^{0}C over one day. The majority of the ligated RNA was produced in the first 30 min after freezing. The maximum ligation yield at this temperature was 25%. The kinetic data of Figure 3.6D was fit by a single exponential. The observed rate constant for ligation was $k_{obs,ligate}$ ~ 0.066/min. A kinetic cleavage reaction was also conducted under similar experimental conditions starting with trace amounts of the 26 nt ^{32}P-labeled P1•P2 substrate and 0.5 μM of ribozyme strand. Similar to the ligation assay, samples were prepared in NTE solvent, placed in a 80 ^{0}C water bath for two minutes, and cooled to 25 ^{o}C before being frozen and incubated at -20 ^{0}C. With no Mg^{2+} present, cleavage in ice was observed over 24 hours, $k_{obs,cleavage}$ ~ .060 min^{-1} (Figure 3.7).

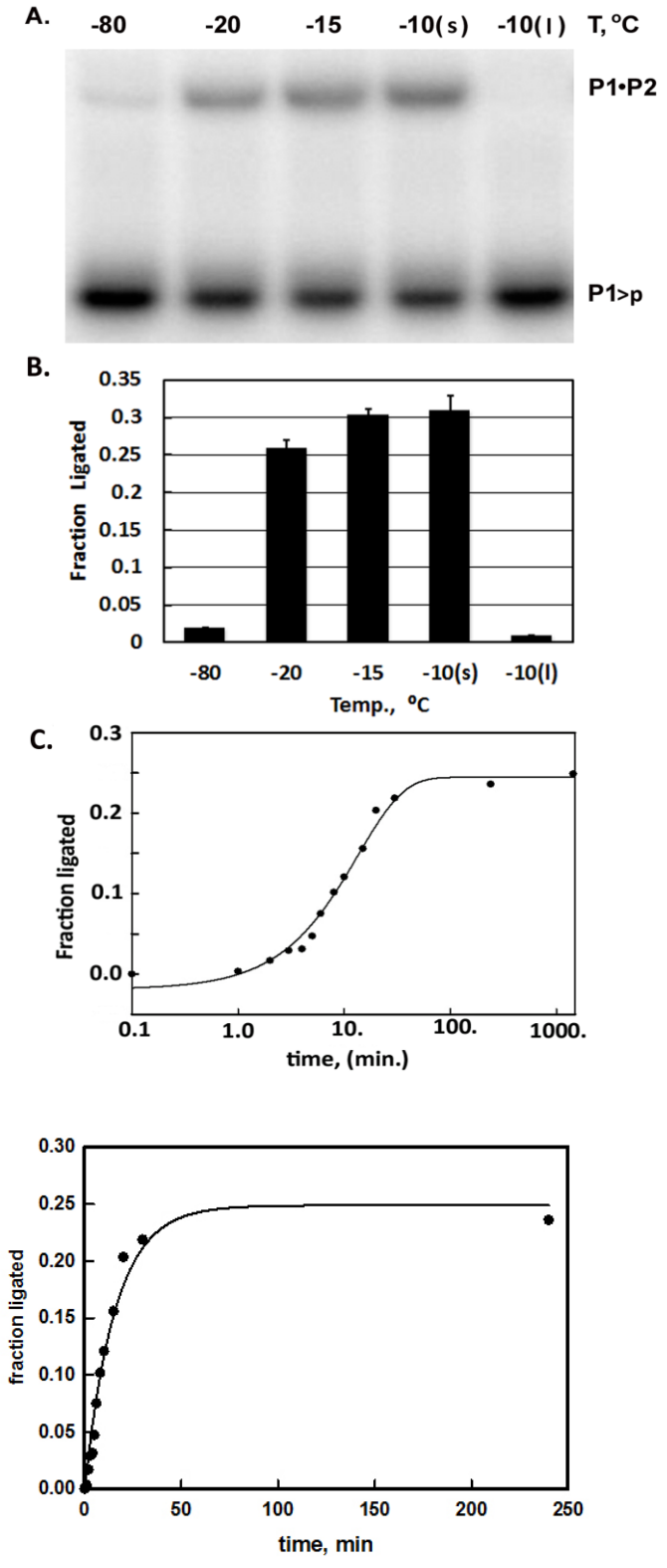

Figure 3.6. A) 12 % denaturing polyacrylamide gel showing ligation of P1>p to P2 by the hammerhead ribozyme under freezing conditions. First four lanes show results for samples quick-frozen and maintained for 24 hrs at -80 ^{0}C, -20 ^{0}C, -15 ^{0}C, and -10 ^{0}C.

The right-most lane shows a sample that was supercooled to -10 ^{0}C and remained a liquid for the 24 hr period. B) Fraction of P1>p ligated to P2 for reactions indicated in A. Bars show the average and standard deviation of three replicates. C) Fraction ligated over a day, demonstrating the long-lived products of ligation. D) Fraction of P1>p ligated to P2 vs time of incubation at -20 ^{0}C ($k_{obs,ligate}$ ~ .066/min).

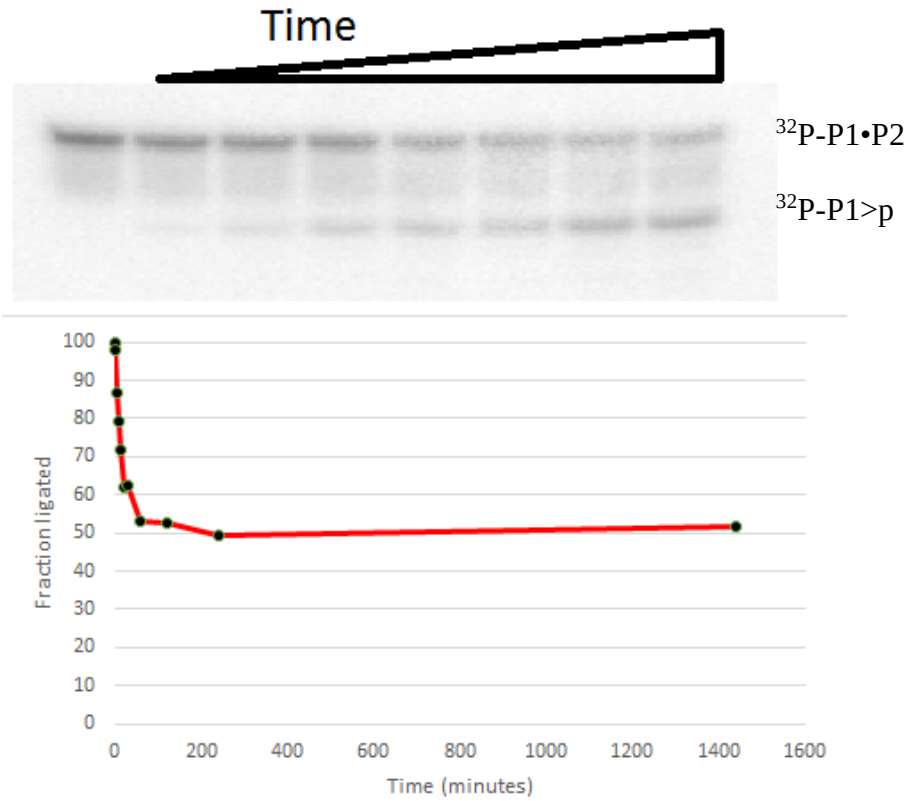

Figure 3.7: Cleavage of the full length substrate by the Schist26 hammerhead in frozen NTE buffer. A) 12% PAGE 7M Urea separating ^{32}P-labeled full length substrate from the ^{32}P-P1>p in a cleavage experiment, incubated at -20 ^{0}C. Individual lanes represent 10 µL aliquots that had been thawed with a formamide stopping buffer after being frozen to initiate the reaction. B) Plot of the fraction of full length P1•P2 remaining at different time points, starting from 100%.

The above experiments were carried out in the absence of divalent cations. If 10 mM $MgCl_2$ was added to the NTE solvent prior to freezing, little ligated product was observed after 24 hrs (~ 1%). This might be due to the high Mg^{2+} concentration in the liquid phase of the eutectic ice-liquid system, and its influence on the 2'3' cyclic phosphate of P1>p. High concentrations of Mg^{2+} have been observed to enhance

hydrolysis of the 2'3' cyclic phosphate of P1>p at room temperature with the presence of the Schist26 complex (Roy 2008).

Influence of dehydration on hammerhead ribozyme ligation

Reduced water activity is one of effects that freezing imposes on the solutes concentrated in the interstitial liquid phase within the crystalline ice. The majority of the water molecules are incorporated into the ice reducing the amount of water available as liquid. Studies on the hairpin ribozyme indicated that dehydration can also promote Mg^{2+} independent ligation (Kazakov et al. 2006). To assess whether dehydration without freezing can induce hammerhead ribozyme ligation, 10 uL aliquots of nM amounts of ^{32}P-labeled P1>p, 0.5 uM of ribozyme, and 2.5 uM of P2 in NTE solvent was centrifuged under vacuum for two hours at 25 ^{o}C. The residue was dissolved in stopping buffer and run on a 12% denaturing polyacrylamide gel. A ligation yield of 7% was obtained. Allowing the residue to remain at 25 ^{o}C for 20 hours prior to adding stopping buffer did not change this value, but some of the P1>p substrate appears to have lost the cyclic phosphate (Figure 3.8). The rate of evaporation also appears to be important; allowing a sample to dry slowly overnight at room temperature by opening the tube cap gave less than 1% ligated product, along with the appearance of the shifted band which may represent the loss of a single phosphate.

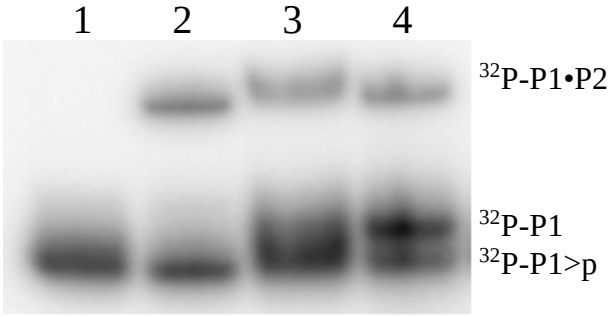

Figure 3.8: 12% PAGE of dehydration-induced ligation of ^{32}P-P1•P2. Lane 1 shows ^{32}P-P1>p as control. Lane 2 is a typical freeze-induced ligation in NTE buffer for 24 hours in -20 ^{0}C. Lane 3 is a 10 uL aliquot that had been speed vacuumed for 2 hours before quenching formamide buffer was added. The last lane is a sample that had also been speed vacuumed for 2 hours, but was left at 25 ^{0}C for 24 hours before it was quenched.

While dehydration increases the concentration of all solutes, we next examined the ligation reaction at 25 ^{o}C in the absence of Mg^{2+} but in the presence of increased monovalent salt concentration. Hammerhead ribozyme cleavage is known to occur in high monovalent cation concentrations in the absence of Mg^{2+} (O'Rear et al. 2001, Murray et al. 1998). A recent crystal structure reveals at least two sites involved in the hammerhead ribozyme catalysis, previously known to only bind to divalent cations, are occupied instead by Na^{+} ions (Anderson et al. 2013). These two sites are important for the coordination of phosphate groups and may be involved in the general acid/base chemistry occurring during hammerhead ribozymecatalysis. With this in mind, we examined the ligation reaction at 25 ^{o}C in the presence of high monovalent salt concentration. Using 4M NaCl instead of the 100 mM NaCl enables ligation at room temperature (Figure 3.9A). The ligation proceeds at $k_{obs,ligate}$ ~ 1.1/min at 25 ^{0}C (Figure 3.9B), slower than Mg^{2+} induced ligation at $k_{obs,ligate}$ ~ 26/min at 25 ^{0}C. Na^{+} cations can apparently replace the Mg^{2+} in the hammerhead RNA. The lower ligation rate with 4M NaCl, implies Na^{+} is not as effective at establishing the conditions for the general acid/base chemistry of ligation.

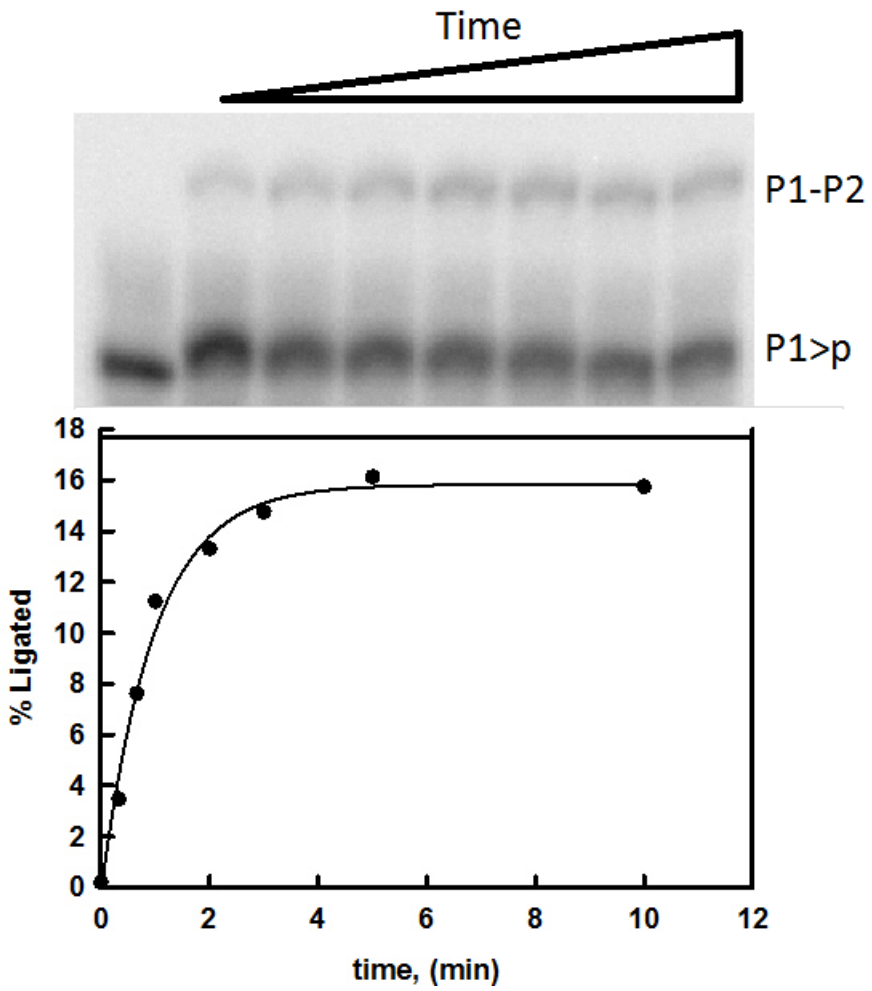

Figure 3.9: Single turnover ligation reaction of the Schist26 hammerhead in 4M NaCl at 25 °C. A) 12% denaturing PAGE separating ^{32}P-P1>p substrate from ligation product ^{32}P-P1•P2. 10 µL aliquots were taken out at different times and quenched with formamide quenching buffer. Reaction was initiated with the addition of ^{32}P-P1>p. B) Graph of percent ligated at different time points, with a $k_{obs,ligate}$ of ~1.1 min^{-1}.

Effect of various solutes in ice

The influence of substituting different cations or anions for Na^+ or Cl^- in the reaction solvent was examined. We note that no freeze-induced ligation was observed if 100 mM NaCl was omitted from the frozen solvent (data not shown). Figure 3.10A shows that substituting Li^+ for Na^+ resulted in a slight increase in ligation yield, while K^+ or NH^{4+} gave a lower yield. The replacement of the chloride anion with other anions produced a range of effects. NaF, NaBr, NaI, and $NaNO_3$ produced lower yields in the

ligation reaction when compared to NaCl (Figure 3.10B). However several anions gave significantly higher yields than chloride.

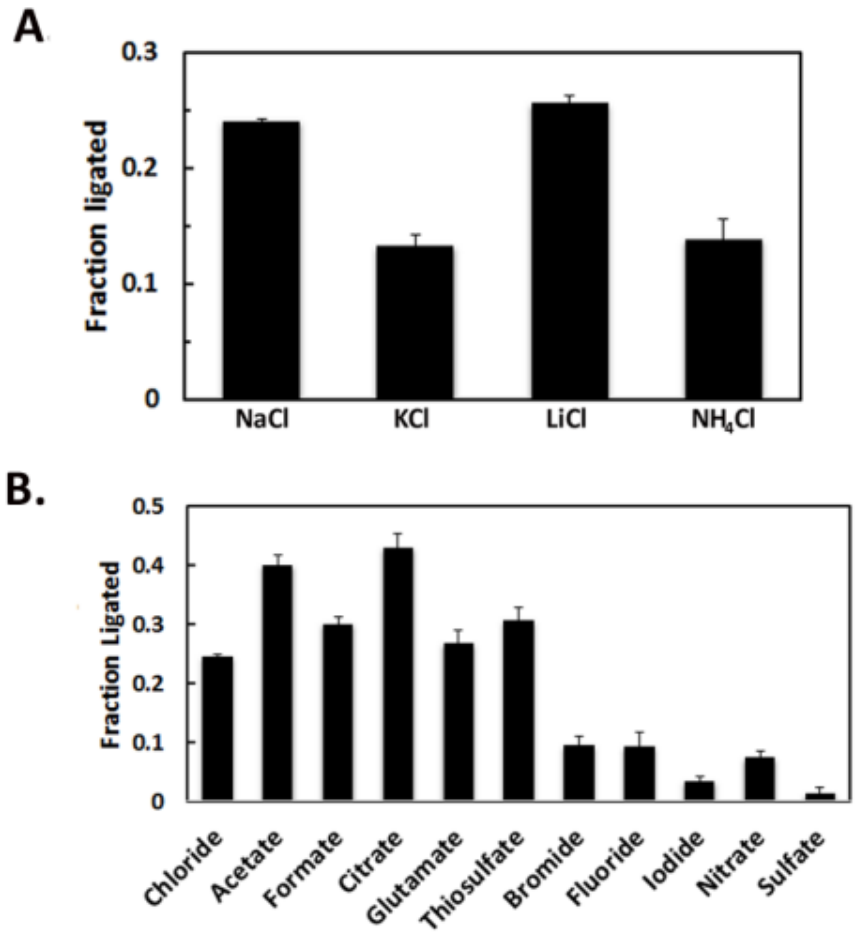

Figure 3.10: Effects of substituting different cations (A) and sodium salt anions (B) for the 100 mM NaCl of the standard NTE solution on the fraction of ligated P1>p. 10 uL samples were quick-frozen and incubated at -20 ^{0}C for 24 hrs. Stopping solution was added and samples loaded into lanes of a 12% denaturing urea-polyacrylamide gel. Bars show average values and standard deviation of three replicate experiments.

The sodium salts of citrate, acetate, formate, and glutamate, all with one or more carboxylate groups, and thiosulfate had ligation yields higher than sodium chloride at -20 ^{o}C (Figure 3.10B). Sodium citrate produced the highest yield, 43%, in the overnight reaction. Although 100 mM of sodium chloride and sodium citrate do not provide the

same concentration of sodium, varying the concentration of sodium citrate between 50 mM to 300 mM had no observable effect on its yield. When the different anions were compared at -15 ^{o}C, where sodium chloride produced its highest ligation yield, the carboxylate anions still had higher yields although by smaller margins than at -20 ^{o}C. When sodium citrate was substituted for sodium chloride in the Mg^{2+}-induced ligation reaction at 25 ^{o}C, no ligation was observed (data not shown). This outcome is likely due to citrate's ability to chelate Mg^{2+} (Adamala and Szostak 2013) which is needed for ligation in solution at moderate ionic strength.

Since osmolytes, polyamines, and amino acids have been shown to influence RNA structure (Lambert and Draper 2007; Higashi et al. 2008; Serganov and Patel 2009), we examined the effect of members of these solute classes on freezing-induced ligation. Solutes added to the canonical NTE solvent were simple sugars (50 mM of glucose, lactose, sucrose, or trehalose); osmolytes (1% glycerol or 100 mM trimethylamine N-oxide), and polyamines (10 mM spermine or spermidine). Freezing-induced ligation yields in the 24 hr reaction were comparable to the control reaction. Except for isoleucine and tryptophan, which reduced ligation yield to about 10%, the addition of the 20 common amino acids at 10 mM did not have a significant effect on ligation.

Thermal cycling increases ligation yield

Periodic freeze-thaw cycling is a plausible scenario for a prebiotic environment. In principle this could enhance the amount of the ribozyme ligated product by promoting turnover of product and substrate and/or refolding of inactive complexes to active complexes. Cycles of freezing and thawing increased the ligation yield of the hairpin ribozyme (Vlassov et al. 2004). Samples were frozen and incubated at -20 ^{o}C for 24 hrs, heated to 70 ^{o}C for 2 min, monotonically cooled to 25 ^{o}C over 15-30 min, and then frozen and incubated again at -20 ^{o}C (Figure 3.11A). After four cycles, ligated product in

the standard NTE solution reached a maximum of 38%, an increase of 13% above one freeze-thaw cycle (Figure 3.11B). If 100 mM sodium chloride was replaced with 100 mM sodium citrate the ligation yield was 43% after the first freeze-thaw cycle, and plateaued at 60% after four cycles. The increase in product with thermal cycling implies that active ribozymes were able to release P1•P2 and bind and ligate other P1>p and P2 substrates. The inability of the ligation yield to approach 100% even with a high ratio of enzyme and P2 strands to P1>p may reflect long-lived inactive ribozymes (Canny et al. 2007). It may also involve the slow rate of opening the 2'3'cyclic phosphate of P1>p as a side reaction of the Schist26 ribozyme strand bound to P1>p, however if this is the case one could expect the ligation yield to decrease upon additional cycling.

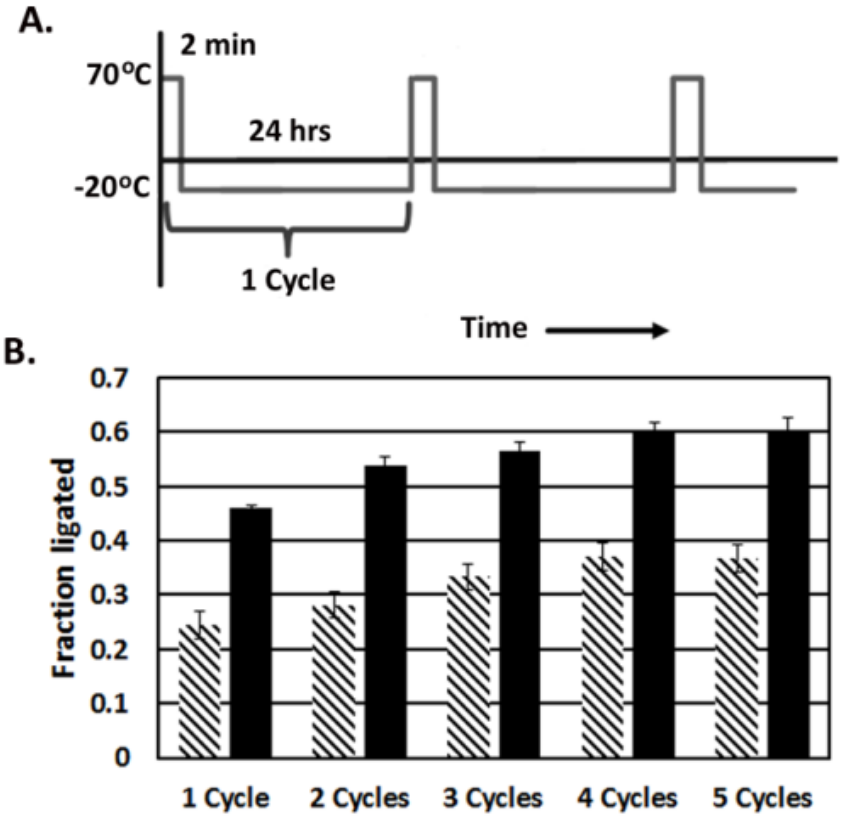

Figure 3.11. A) Schematic of the thermal cycling experiment. Samples were heated to 70 ^{0}C for 2 min, cooled for 15-30 min at 25 ^{o}C, then quick-frozen and incubated at -20 ^{o}C for 24 hrs. Cycle was repeated. B) Results of ligation reaction after increasing rounds of thermal cycling. The diagonal cross hatch bars are with samples in the standard NTE

solution. The black bars are results with 100 mM sodium citrate replacing 100 mM sodium chloride of NTE solution.

Effect of pH on hammerhead ligation

The influence of the solvent pH (measured at 25 °C) on the freezing-induced ligation yield was also examined. The pH of the NTE solvent from 7.0 to 9.0 did not have a significant effect on ligation, probably due to how the pH of Tris buffer increases when the solution is frozen (Figure 3.12). An alternative method to generating the P1>p without the use of the hammerhead ribozyme, is the use of carbodiimide in a MES buffer pH 5.5 (Hertel 1994). To assess ligation at pH 5.5 and 8.0 in the same buffer, the 50 mM Tris buffer of the NTE solvent was replaced with 50 mM sodium phosphate. Virtually no ligation product was detected at pH 5.5 at any tested temperature while the yield was highest at 24% for the phosphate buffer at pH 8.0 in -15 °C (data not shown).

Changes in buffer pH in ice

The pH of a solution does not stay the same at all temperatures. Although the pH of our Tris starts out as 8.0, freezing the solution will change that initial pH. Even lowering the temperature will raise the pH; a 50 mM pH 8.0 Tris buffer at 37 °C, will rise to pH 8.3 at 25 °C, and then continue to increase to pH 8.9 at 5 °C (Sambrooks and Russell 2001)). No data for pH of Tris in ice was found, but it would be reasonable to think that the indirect relationship between temperature and Tris pH is maintained even in frozen conditions. We tested the pH by freezing pH strips from J.T. Baker, Germany in various frozen buffers (Figure 3.12). As expected, a pH 8.0 Tris buffer increases in pH by one or two. In contrast, the pH of PIPES remains stable in ice and did not change.

A

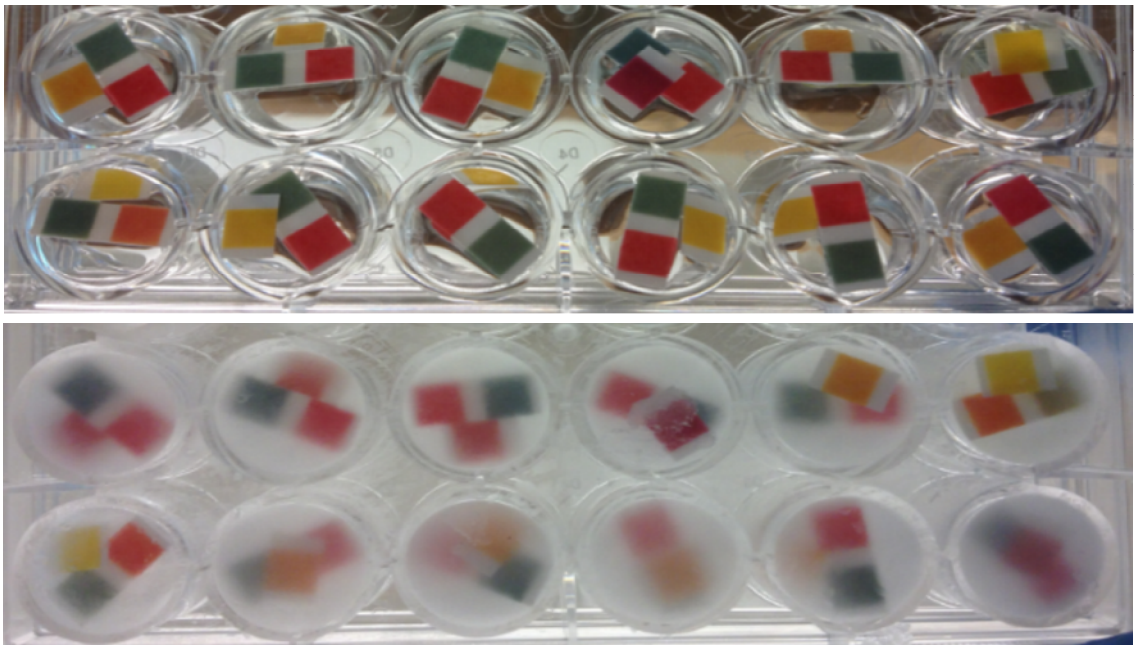

B

Cell	Solution	25 °C/ -20 °C
1	pH standard 7.0	~7/~6
2	pH standard 8.0	~8/~8
3	pH standard 10.0	~10/~10
4	50 mM Tris pH 8.0, 100 mM NaCl	~8/~9
5	50 mM Tris pH 8.0, 100 mM NaBr	~8/~9
6	50 mM Tris pH 8.0, 100 mM NaFl	~8/~10
7	50 mM Tris pH 8.0, 100 mM NaI	~8/~10
8	50 mM PIPES pH 8.0, 100 mM NaCl	~8/~8
9	50 mM PIPES pH 8.0, 100 mM NaBr	~8/~8
10	50 mM PIPES pH 8.0, 100 mM NaFl	~8/~8
11	50 mM PIPES pH 8.0, 100 mM NaI	~8/~8
12	Millipore filtered water	~6/~6

Figure 3.12: pH measurement of various buffers before and during freezing at -20 °C. A) Top panel of twelve cells filled with buffers and pH strips. Bottom panel is the same twelve cells after being frozen at -20 °C for three hours. Color change of the pH strips in frozen solution indicate a pH change. B) Table of cells and the buffers tested. Tris buffer shows an increase in pH when frozen. Cell numbers 1 to 6 represent the top row of cells in the tray and 7 to 12 refer to the bottom row.

Discussion

The results presented in this study demonstrate that the *Schistosoma* hammerhead can efficiently ligate RNA oligomers in frozen solution in the absence of Mg^{2+}. Under single turnover conditions, freezing induced ligation produced yields up to 43% after one freeze-thaw cycle, and 60% if several freeze-thaw cycles were employed to denature and refold the ribozyme-substrates complex. These values are significantly higher than the maximum ligation yield of 23% reported for this ribozyme in solution.

The increase in ligation over several days of freeze-thaw cycles also indicates that the 2'3' cyclic phosphate group on P1>p is relatively stable under the conditions employed. This was not the case for the Mg^{2+}-induced ligation reaction at 25 ^{0}C (Figure 3.4), or when 10 mM Mg^{2+} was present in the frozen solution. At 25 ^{0}C the ligated product slowly decreased after reaching a maximum in ~20 seconds, and in frozen solution no product was observed after an incubation of 24 hrs. These observations may be due to the slow opening of the 2'3'cyclic phosphate as a side reaction of HHR ligation in the presence of high concentrations of Mg^{2+} (Roy 2008).

Freezing-induced ligation in the absence of Mg^{2+} is much slower than ligation in solution with Mg^{2+}, but the product was more stable. The ligation activity of the HHR in the eutectic ice-liquid environment appears to result from the high concentration of monovalent salts in the liquid phase. When NaCl was removed from the NTE solvent, freezing-induced ligation was not observed. Freezing a solution crystallizes the majority of the water, concentrating the RNA and other solutes in the remaining liquid phase and reducing the water activity of this environment (Kanavarioti et al. 2001; Trinks et al. 2005). The hammerhead ribozyme is known to cleave in high monovalent salt concentrations in aqueous solution (Murray et al. 1998; Curtis and Bartel 2001) and here we show that it can ligate with high salt concentrations in the absence of divalent cations.

Although lowering solution temperature shifts hammerhead cleavage-ligation equilibrium toward ligation when Mg^{2+} is present (Stage-Zimmermann and Uhlenbeck 2001), incubating reaction samples below 0 ^{o}C without ice formation produced very little ligation (Figure 3.5A).

Experiments with the hairpin ribozyme suggested that dehydration of RNA by the concentrated salts is a major factor in this ribozyme's ligation activity in ice (Kazakov et al. 2006). For the hammerhead ribozyme we observed that dehydrating and concentrating a reaction sample by vacuum centrifugation at 25 ^{0}C produced ligated products in support of this interpretation. However the rate of dehydration was important. When a similar sample was allowed to slowly evaporate overnight at 25 ^{0}C the amount of ligated product was negligible.

Ligation by the hammerhead in frozen solution was observed using a variety of solvent conditions with generally similar yields. Notable exceptions were the higher product yields obtained when sodium chloride was replaced with sodium salts of formate, acetate, and citrate, anions with carboxylate groups, and with sodium thiosulfate. The favorable effects of the above anions in the eutectic system may be due to a combination of factors.

It has been demonstrated that hydrolysis of the RNA backbone by a ligand can be influenced by a carboxylate ion acting as a general base (Endo et al. 1996). In the generally accepted model of the cleavage reaction by the hammerhead, the 2'-OH of the G8 nucleoside acts as a general acid interacting with the oxygen on the scissile phosphate P1.1, while N1 of the G12 base acts as a general base abstracting the hydrogen from the 2'-OH of the C17 nucleoside to generate an oxygen nucleophile (Han and Burke 2005). Similarly, the ligation reaction would require a general acid and a general base but in a different sequence of events. Thiosulfate and the three carboxylate anions; formate, acetate, and citrate all have pK_a values well below the pH 8.0 of the Tris buffer. All of these anions would be expected to be deprotonated. If anions bind to an appropriate

RNA site (Auffinger et al. 2011), they may serve as a general base and enhance the ligation reaction (Figure S3.2).

The above anions may also favor ligation activity by binding water molecules in the vicinity of the HHR and promote ligation through dehydration. Formate, acetate and citrate have positive Jones-Dole viscosity B coefficients (0.052, 0.250, 0.75) a measure of the strength of ion-water interactions relative to water-water interaction in solution (Collins 2006) . Thiosulfate, which also enhanced ligation yield, also has a positive B coefficient of .170 (Figure S3.3) (Wolf 1966). Most anions that did not enhance ligation have negative B coefficients (I, Br, NO_3) (Collins 2006).

Two anions that did not follow the above trend were fluoride and sulfate. Fluoride has a positive B coefficient of 0.10 but its ligation yield was only 9%. Sulfate is a strongly hydrated anion with B= 0.210, but it gave a very low ligation yield (Figure 3.9B). However the outcomes with sodium fluoride and sodium sulfate may be related to their relatively low solubility compared to the sodium salts that enhanced ligation. The sodium salts of chloride, citrate, acetate, formate and thiosulfate at 0 ^{0}C have solubility values per 100 g water $\geq$ 32 g, while sodium sulfate is 4.9g and sodium fluoride is 3.6g (Gao et al. 2012, Haynes 2013, Seidell and Linke 1958). Sodium fluoride and sodium sulfate may precipitate in the liquid phase of the frozen solution. Figure S3.3 plots the anion B coefficients vs. ligation yields obtained in Figure 3.10. The correlation between the hydration strength and solubility characteristics of the anions and their influence on ligation suggests that these two factors are important in freezing-induced ligation by the HHR.

Figure S3.1: Reaction scheme of the Schist26 HHR reversible cleavage and ligation reaction with a branching irreversible side reaction for P1-p (Adapted from Canny et al. 2007).

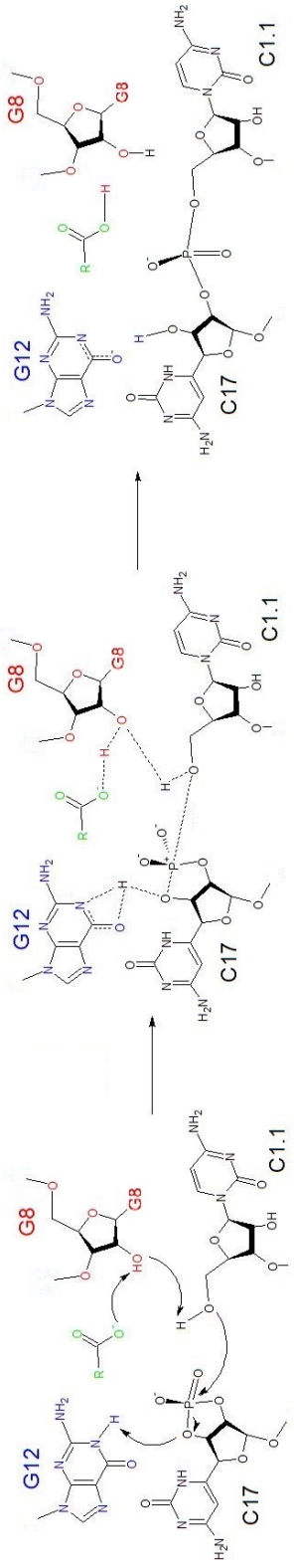

Figure S3.2: Proposed mechanism for hammerhead ligation with a carboxylate participating in the acid/base chemistry during catalysis (Adapted from Chi et al. 2008).

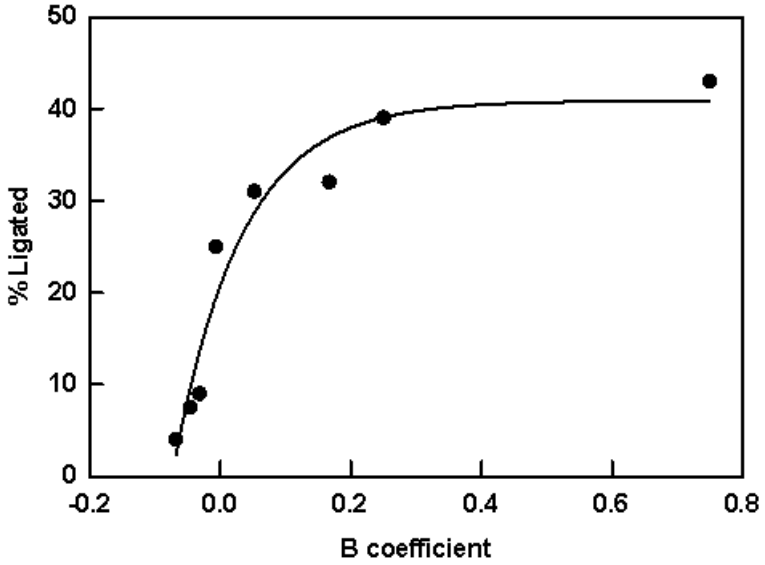

Figure S3.3: Plot Percent Ligated by Schist26 hammerhead versus Jones-Dole viscosity B coefficients.

CHAPTER 4

EFFECT OF MUTANT P1 AND P2 ON HAMMERHEAD RIBOZYME LIGATION IN ICE

Introduction

The hammerhead enzyme is a catalytic RNA first found in the tobacco ringspot virus (Prody et al. 1986) and then later, among other organisms, in schistosomes (Chartrand et al. 1995). It is a motif with a conserved catalytic core with three stems. The hammerhead ribozyme being tested is the Schist26 from the parasite *Schistosoma mansoni*; it has longer stems than the minimal ribozyme to include the hairpin loop in Stem II and the internal loop at Stem 1 (Canny et al. 2007) (Figure 4.1). The hammerhead ribozyme can catalyze reversible transesterification reaction which produces two cleavage products: P1 with a 2'3' -cyclic phosphate and a P2 with a 5' OH. For efficient catalysis, both ligation and cleavage, the loop-loop interactions between Stems I and II is crucial and is supported by the stable basepairing of those helices (De la Pena et al. 2003, Khorova et al. 2003). It was three years later when the three-dimensional structure of a natural hammerhead ribozyme showed that the terminal loop of Stem II non-canonically base pairs with Stem I's internal loop (Martick and Scott 2006). While Stem III requires no loops, it does require a minimum of four base pairs for efficient cleavage activity (Canny et al. 2007).

The results presented in the last chapter demonstrate that the *Schistosoma* Schist26 can efficiently ligate RNA oligomers in frozen solution in the absence of Mg^{2+}. Under single turnover conditions, freezing induced ligation produced yields up to 43% after one freeze-thaw cycle, and 60% if several freeze-thaw cycles were employed to

denature and refold the ribozyme-substrates complex. These values are significantly higher than the maximum ligation yield of 23% reported for this ribozyme in solution. The increase in ligation over several days of freeze-thaw cycles also indicates that the 2'3' cyclic phosphate group on P1>p is relatively stable under the conditions employed. This was not the case for the Mg^{2+}-induced ligation reaction at 25 ^{0}C (Fig.2), or when 10 mM Mg^{2+} was present in the frozen solution. At 25 ^{0}C the ligated product slowly decreased after reaching a maximum in ~20 seconds, and in frozen solution no product was observed after an incubation of 24 hrs. These observations may be due to the slow opening of the 2'3'cyclic phosphate as a side reaction of Schist26 ligation in the presence of high concentrations of Mg^{2+} (Roy 2008).

Freezing-induced ligation in the absence of Mg^{2+} is much slower than ligation in solution with Mg^{2+}, but the product was more stable.

Mutant P1 and P2 fragments were designed to test the base pairing requirement of the Schist26 hammerhead ligation in ice. Three P1 mutant sequences were examined. The P1-M mutant has one guanine switched to an adenine and the P1-7 mutant is missing three nucleotides from the 5' end (Figure 4.1). Of the three P1 mutants examined, P1-5 provides the most stringent assessment of the base pairing requirements in ice versus in liquid. Although a minimum of four base pairs in Stem III was sufficient for efficient cleavage of the P1•P2 substrate at 25 ^{o}C with Mg^{2+}, the ligation reaction required more than five base pairs between the P1 and E strand. Canny et al (2007) showed that P1-5 is unable to ligate to P2 at 25 ^{o}C and 10 mM $MgCl_2$ due to the high dissociation rate of P1-5 compared to the ribozyme's ligation rate (Canny et al. 2007). The P2-5N mutants consisted of a pool of P2 fragments with a mixture of all four bases at five positions that normally form Watson Crick base pairs of Stem I. Mismatches at these positions could also possibly affect the tertiary interactions between Stems I and II (Figure 4.1).

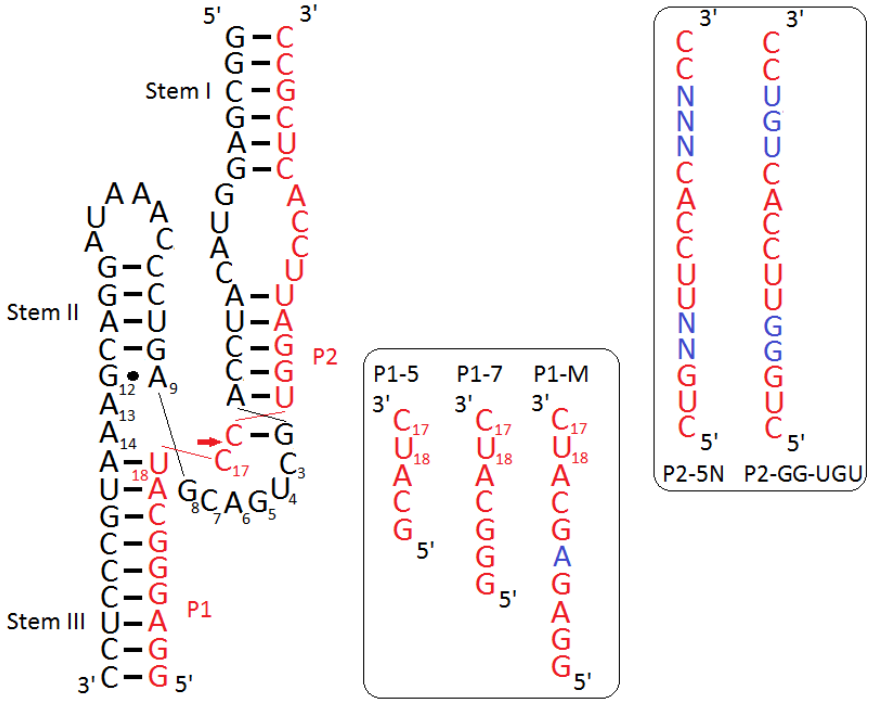

Figure 4.1: Secondary structure of the Schist26 hammerhead ribozyme from *Schistosoma mansoni* with its ligation substrates P1 and P2. Black symbolizes the ribozyme or E strand and red letters indicate substrates, both wild type and mutants. Blue letters represent the base substitutions with N = A,G,C, or U (Adapted from Canny et al. 2007).

Materials and Methods

RNA oligomers and modification

The 49-nt *S. mansoni* hammerhead ribozyme strand (E) was generated by in vitro transcription of a 68 bp DNA containing the template sequence joined to a T7 promoter. The DNA template strands (IDTDNA) were characterized by denaturing gel electrophoresis to verify purity. They were heated to 90 ^{0}C for two min and slowly cooled to form a duplex before being transcribed with an Ambion MEGAscript T7 kit. The resulting RNA was gel purified. Other RNA oligomers were chemically synthesized (IDTDNA), characterized by denaturing gel electrophoresis and modified if necessary as described below. They were P1: 5'GGAGGGCAUCp3', P2: 5'CUGGAUUCCACUCGCC3', P1•P2:

5’GGAGGGCAUCCUGGAUUCCACUCGCC3’, P1-7: 5’GGGCAUCp3’, P1-5: 5’GCAUCp3’, P1-M: 5’GGAGAGCAUCp3’, pP1: 5’pGGAGGGAUCp3’, and P2-5N: 5’CUGNNUUCCACNNNCC3’ where N represents a mixture of the four bases A,C,G. U. Figure 4.1 displays the E and P1•P2 strands assembled as the *S. mansoni* hammerhead ribozyme, and some of the other oligomers.

The P1>p strand, which is the P1 sequence with a 2’3’ cyclic phosphate at its 3’ end, was generated either from hammerhead ribozyme-facilitated cleavage of P1•P2, or by treatment of P1 with 1-ethyl-3-[3-dimethylaminopropyl] carbodiimide (EDC). Cleavage of 10 pmoles of P1•P2 followed after it was 5’ ^{32}P-end labeled using T4 polynucleotide kinase (3’phosphatase minus) and ^{32}P-γATP in a 50 ul reaction. 100 pmoles of the E strand was added to 5’ end-labeled P1•P2 in kinase buffer, and the reaction cycled four times for 2 min at 70 ^{0}C and 20 min at 25 ^{0}C. To generate a 2’3’ cyclic phosphate at the 3’ end of P1 and its mutant derivatives, the RNA was incubated with 50 mM EDC, 100 mM MES buffer pH 5.5 for 1 hr at 37 ^{0}C (Hertel et al. 1994). P1>p and its mutant derivatives were purified from their unmodified substrates by 20% denaturing PAGE, excised, and ethanol precipitated with glycogen.

Ligation reactions

A typical master mix contained 0.5 µM ribozyme strand, 2.5 µM P2 fragment, and trace amounts of ^{32}P-labeled P1>p in a 100 uL solution of 50 mM Tris pH 8.0, 100 mM NaCl, and 0.1 mM EDTA (NTE buffer). Sodium mesh chelating resin (Sigma) was used to remove trace amounts of Mg^{2+} in buffers and reaction mixtures. The chelating resin was included in the RNA annealing step in which the reaction mixture was heated to 80 ^{o}C for 2 min and then allowed to cool at 25 ^{o}C for 30 min. The resin was removed by filter centrifugation. Freezing-induced ligation was initiated by freezing 10 uL aliquots in a -80 ^{o}C ethanol bath for 1 min and rapidly transferring the reaction to a temperature controlled polyethylene glycol-water bath. The quick freezing step avoided variations in

the rate of freezing for timed reactions. Samples placed directly in the bath gave the same results in overnight reactions. Ligation reactions in solution at 25 ^{o}C were initiated by adding $MgCl_2$ to the master mix to give a final concentration of 5 mM. Reactions were halted by adding cold stopping solution of deionized formamide and 20 mM EDTA with bromophenol blue and xylene cyanol in a 4:1 ratio to the sample. Products were run on a 12% denaturing polyacrylamide gel (7 M urea) and analyzed with a GE Typhoon Imager and Fuji Multi Gauge Imaging software.

Sequencing of ligation products using P2-5N substrate

A 200 uL reaction with 1µM of pP1>p, 5 µM of hammerhead ribozyme strand, and 25 µM of P2-5N in 100 mM sodium citrate, 0.1 mM EDTA, and 50 mM Tris (pH 8.0), was heated to 70 ^{o}C for 1 min and subsequently cooled for 15-30 min at 25 ^{o}C before being frozen at -20 ^{0}C for 24 hrs. The reaction was heated and then quick-frozen 3 additional times. The ribozyme strand was removed by heating the reaction at 80 ^{o}C for 1 min with 100 uL of a 5' biotinylated complementary DNA strand (5'-AGGGCATTTCGTCCTATTTGGGACTCGTCAGCTGGATGTACCTCGCC -3') at 50 µM and cooled to 25 ^{0}C prior to adding streptavidin beads to remove the ribozyme strand-DNA hybrid. Residual DNA was removed by digesting the sample with DNase (Ambion TURBO DNase). The 26nt RNA ligation products were gel purified and precipitated with EdgeBio Quick-Precip Plus solution.

A cDNA library was prepared for Illumina sequencing from the 26 nt RNAs with the NEBNext Small RNA Library Preparation Kit (NEB Inc). The amplified cDNA was gel purified and verified for purity by observing only a single band in a 5% native PAGE, correct length of ~145bp, and concentration using an Agilent model 2100 Bioanalyzer. Single read sequence data was obtained by LCSciences Inc. A Q score of 30 or higher was observed for 97% of base reads. Sequencing was also carried out with Georgia Tech's Illumina HiSeq2000. Data from each run were filtered and sorted and both gave

essentially the same hierarchy of RNA sequences. The Perl script used to analyze the sequence data, and the 100 most frequently encountered sequences are given in Supplementary Figure S4.1 and Table S4.1.

Results

The effect of mutations in P1 and P2 on ligation in frozen solution

Efficient ligation is dependent on low dissociation rates compared to the ligation rate, and freezing the hammerhead complex may lower the dissociation rates to allow ligation of short substrates. To explore how the stability of the Stem III duplex influences ligation, three P1 homologs were synthesized and treated with EDC to generate 2'3'cyclic phosphates at their 3' ends. All three of the modified P1 sequences could be ligated to P2 in frozen solution (Figure 4.2). P1-7 and P1-M gave similar ligation yields, averaging 24% for the five solvents employed. P1-5 ligated to P2 with an average ligation yield of 14% over all tested solvents.

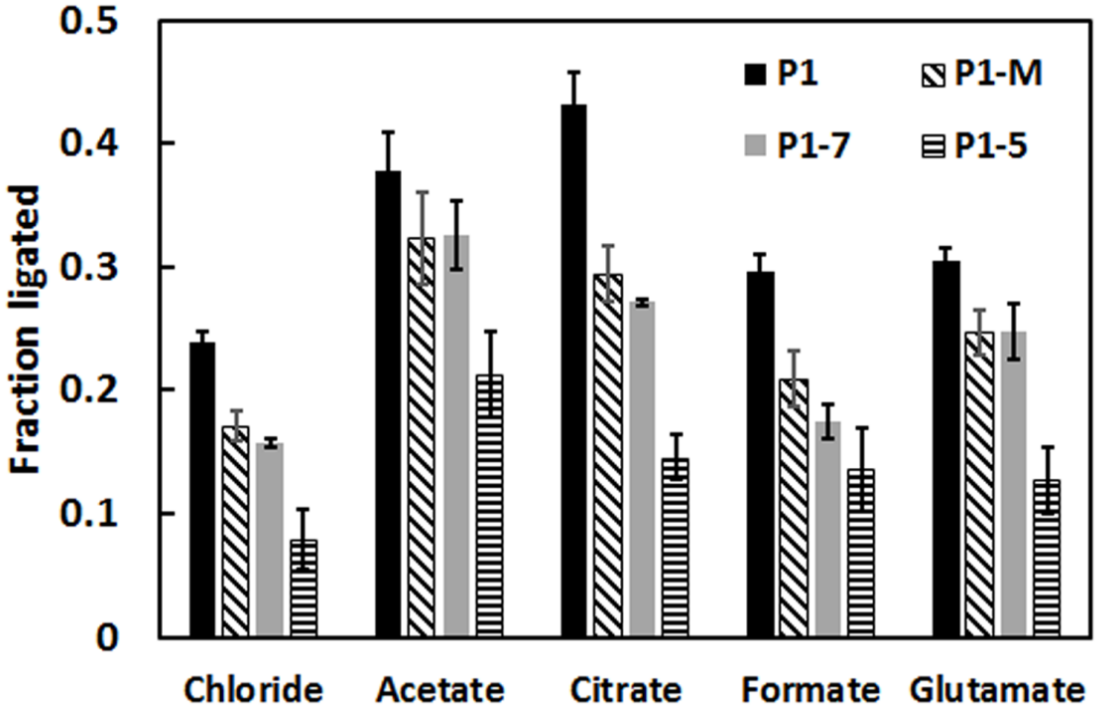

Figure 4.2. Hammerhead ribozyme ligation using various P1 constructs. Each has the 2'3' cyclic phosphate at their 3' ends. Average values of fraction ligated and standard deviations are based on three to four replicate experiments. All samples were incubated at -20 ^{0}C for 24 hrs prior to 12% denaturing PAGE analysis. Effects of various sodium salts at 100 mM in 50 mM Tris (8.0) + 0.1 mM EDTA solution are shown.

We next examined the influence of mismatches in the duplex formed by the ribozyme strand and P2. Freezing induced ligation of P1>p with P2-5N in NTE solvent gave a yield of ~12% in a 24 hr reaction at -20 ^{o}C. Since 1024 different sequences are expected in the pool of P2-5N oligomers, more than just the wild type P2 was ligated to P1. The P1•P2-5N ligation product was prepared for sequencing as described in Material and Methods, purified by gel electrophoresis and a cDNA library prepared for Illumina sequencing. 70 out of the 1024 possible P2 sequences were represented in ligated products at greater than 1000 read counts per million. The 100 most frequently encountered sequences (Table S4.1) displayed a consensus sequence that differed at three of the five randomized positions from the wild type GA-UCG sequence. The consensus bases and the percentages at which they appeared were GG-U(G/U)U with percentages of

58%, 42%, 58%, 38%, and 36% respectively (position 23 had 38% G and 38% U and is thus designated G/U) (Figure 4.3).

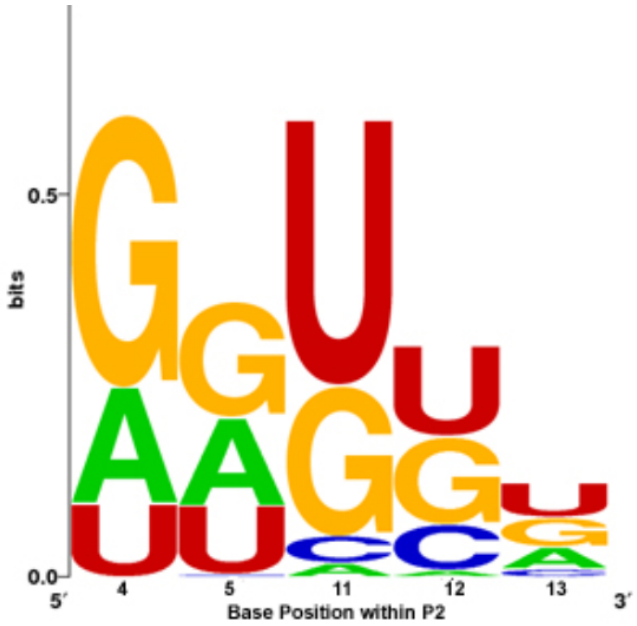

Figure 4.3: Letters are scaled to how much that base is represented in the Hiseq runs. The dominant bases appear to be G in the fourth position of the P2-5N (fourteenth base on the full length product), G in the fifth (fifteenth), U in the eleventh (21st), U or G on the twelfth (22nd), and finally U on the thirteenth (23rd).

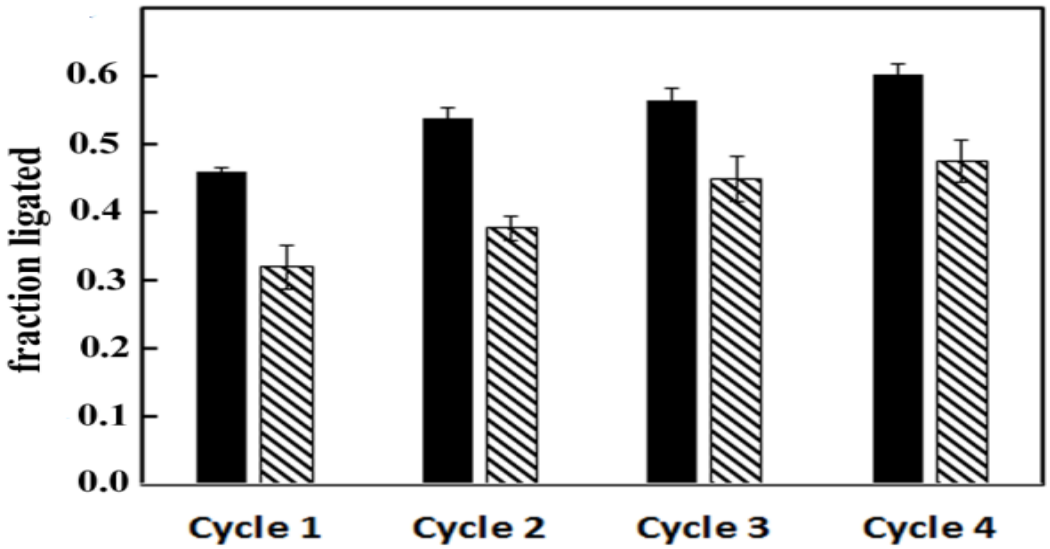

Fig 4.4: Fraction of P1>p ligated to wild type P2 (filled bars) or P2-GG-UGU (diagonal hatch bars) induced by freezing to -20 ^{o}C with sodium citrate, after multiple thermal cycles as described in Figure 3.10.

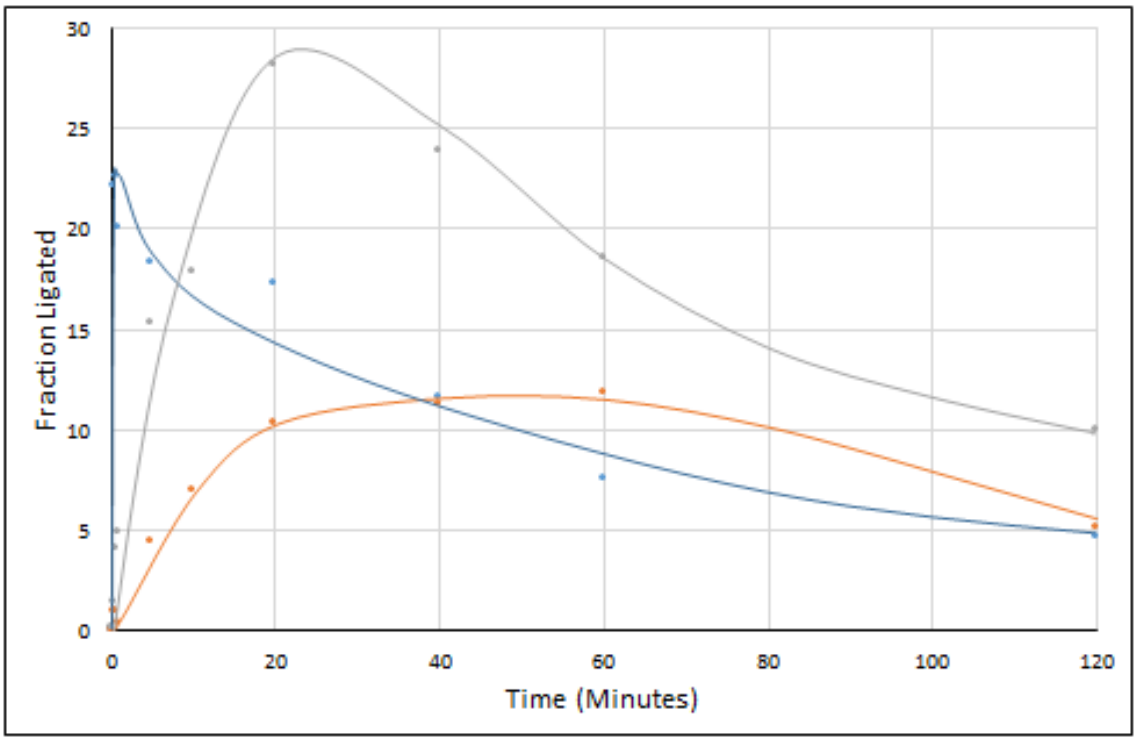

Figure 4.5: Comparison of Mg^{2+} induced ligation reaction at 25 ^{o}C in NTE solution with 5 mM Mg^{2+} as described in Materials and Methods. Dashed line corresponds to P1>p and P2, while solid line corresponds to P1>p and P2-GG-UGU.

The wild type P2 sequence was surprisingly not the most frequently encountered sequence among the ligated products (see Discussion). The most frequently encountered sequence, P2-GG-UGU (Figure 4.1) is consistent with the above consensus sequence. It was tested individually in a freezing-induced ligation reaction. This sequence was less efficiently ligated than the wild type P2 sequence, but gave substantial yields of ~30% in 24 hrs, and ~45% after four thermal cycles (Figure 4.4). A point worth noting with regard to the P2-GG-UGU oligomer was its behavior in the Mg^{2+} induced ligation reaction at 25 ^{o}C. Unlike P2, which reached a plateau within 20 seconds, P2-GG-UGU ligated to P1>p at a much slower rate, but reached a slightly higher maximum in 30 min at 25 ^{0}C (Figure 4.5). A fit to a single exponential equation for data obtained for times between 0 and 30

minutes gave a value of k_{obs} ~ 0.13 min^{-1} for P2-GG-UGU. For the P2 sequence k_{obs} at 25 ^{0}C was in the range of 10 to 40 min^{-1} for times between 0 and 5 minutes. With its 1000+ mutants, P2-5N k_{obs} between 0-10 min is about 0.09 min^{-1} at 25 ^{0}C.

Discussion

The ability of the HHR to ligate mutated P1 and P2 substrates in frozen solution indicates that this environment has a reduced requirement for ribozyme-substrate Watson-Crick base pair stability compared to ambient temperatures. The five-nucleotide substrate P1-5, which showed no ligation at 25 ^{o}C (Canny et al. 2007) was ligated to P2 in frozen solution. 70 out of the 1024 possible P2 sequences were represented by 10^3 or more read counts per million. The observation that the wild type P2 sequence was not the most highly represented sequence in the ligated P1•P2-5N ensemble (Table S4.1) was unexpected. When assessed individually in the eutectic environment, the wild type P2 sequence ligated more efficiently to P1 than the P2 sequence with the highest read counts, P2-GG-UGU (Figure 4.4). Several factors, in addition to ribozyme-substrate stability, are likely to have contributed to the order of the P1•P2-5N oligomers found by read counts. The five randomized positions of P2-5N may not have had equal molar amounts of the four bases due to different coupling efficiencies of the RNA bases (A. Conklin, Integrated DNA Technologies, personal communication). A less likely factor is PCR amplification bias. Hairpin-like structures predicted by RNA Structure (Reuter and Mathews 2010) for some P1•P2-5N sequences linked to the 5' adapter of the library kit could contribute to this. Another factor is the pool of P2-5N itself. The only difference in protocol between the ligation reaction used for library preparation and the reactions for Figure 4.4 is the concentration of RNA. P2-5N makes up the bulk of the total RNA

concentration with 25 μM. The wild type P2 may have bound to mutant P2s instead of the ribozyme, resulting in reduced read counts.

Supplementary

Table S4.1: Top 100 most frequent sequences pulled from the Hiseq runs of Schist26 ligation with P2-5N. The numbers associated with each sequence is the number of counts per million.

364712.8	GGAGGGCATCCTGGGTTCCACTGTCC
170857	GGAGGGCATCCTGGGTTCCACTGGCC
61995.38	GGAGGGCATCCTGGGTTCCACTGACC
44902	GGAGGGCATCCTGAGTTCCACTGTCC
38530.5	GGAGGGCATCCTGGGTTCCACGTTCC
36783.75	GGAGGGCATCCTGTGTTCCACTGTCC
20198.88	GGAGGGCATCCTGTATTCCACTGTCC
17827.5	GGAGGGCATCCTGGTTTCCACTGTCC
17551.88	GGAGGGCATCCTGTTTTCCACTGTCC
13461.38	GGAGGGCATCCTGAGTTCCACTGGCC
11252	GGAGGGCATCCTGGGTTCCACTTGCC
10499.5	GGAGGGCATCCTGGGTTCCACGTACC
8918.75	GGAGGGCATCCTGGATTCCACTGGCC
8409.75	GGAGGGCATCCTGGGTTCCACTTTCC
7428.5	GGAGGGCATCCTGGGTTCCACGCGCC
7141.125	GGAGGGCATCCTGGATTCCACTGTCC
6833.75	GGAGGGCATCCTGAATTCCACTGTCC
6478.625	GGAGGGCATCCTGAGTTCCACTGACC
6429.125	GGAGGGCATCCTGGTTTCCACTGGCC
5880.75	GGAGGGCATCCTGGGTTCCACGTGCC

Table S4.1 continued

5302.375	GGAGGGCATCCTGGTTTCCACGTTCC
5276	GGAGGGCATCCTGGGTTCCACGCTCC
4978.75	GGAGGGCATCCTGTTTTCCACTGGCC
4758.75	GGAGGGCATCCTGGGTTCCACGGTCC
4739.5	GGAGGGCATCCTGGGTTCCACTCGCC
4428.375	GGAGGGCATCCTGGGTTCCACTGCCC
3979.5	GGAGGGCATCCTGGTTTCCACTGACC
3735.625	GGAGGGCATCCTGGGTTCCACGCACC
3595.625	GGAGGGCATCCTGGTTTCCACTCGCC
3586.125	GGAGGGCATCCTGTTTTCCACTGACC
3527.375	GGAGGGCATCCTGGTTTCCACTTTCC
3083.125	GGAGGGCATCCTGTGTTCCACTGGCC
3052.25	GGAGGGCATCCTGGGTTCCACCTGCC
2853.5	GGAGGGCATCCTGGGTTCCACTCTCC
2799.375	GGAGGGCATCCTGGATTCCACGCGCC
2799.25	GGAGGGCATCCTGAATTCCACTGGCC
2783.5	GGAGGGCATCCTGGGTTCCACTAGCC
2623.625	GGAGGGCATCCTGAATTCCACTGACC
2473.75	GGAGGGCATCCTGTATTCCACTGGCC
2311.125	GGAGGGCATCCTGATTTCCACTGACC
2265.375	GGAGGGCATCCTGTATTCCACTTTCC
2060	GGAGGGCATCCTGGGTTCCACCTTCC
2027.875	GGAGGGCATCCTGATTTCCACTGTCC
2001.25	GGAGGGCATCCTGGATTCCACGTTCC
1973.625	GGAGGGCATCCTGGGTTCCACGTCCC

Table S4.1 continued

1957.75	GGAGGGCATCCTGGGTTCCACCGTCC
1933.125	GGAGGGCATCCTGGATTCCACTGACC
1791.875	GGAGGGCATCCTGATTTCCACTGGCC
1744.5	GGAGGGCATCCTGGTTTCCACGCTCC
1656.875	GGAGGGCATCCTGGTTTCCACTTGCC
1621.625	GGAGGGCATCCTGTGTTCCACTGACC
1574.75	GGAGGGCATCCTGGGTTCCACTTACC
1468.75	GGAGGGCATCCTGGGTTCCACGGGCC
1409	GGAGGGCATCCTGAGTTCCACGTTCC
1391.375	GGAGGGCATCCTGGTTTCCACGCGCC
1385	GGAGGGCATCCTGGGTTCCACTATCC
1382.75	GGAGGGCATCCTGGATTCCACGTACC
1380.625	GGAGGGCATCCTGAATTCCACGTACC
1353.375	GGAGGGCATCCTGGTTTCCACTGCCC
1308.25	GGAGGGCATCCTGGATTCCACTTGCC
1245.25	GGAGGGCATCCTGAATTCCACTTTCC
1201.25	GGAGGGCATCCTGGATTCCACGCACC
1141.875	GGAGGGCATCCTGGTTTCCACGTACC
1135.375	GGAGGGCATCCTGAATTCCACGCACC
1127.375	GGAGGGCATCCTGGGTTCCACCGGCC
1106.125	GGAGGGCATCCTGAATTCCACTTGCC
1067.5	GGAGGGCATCCTGAATTCCACTTACC
1061.25	GGAGGGCATCCTGGATTCCACGCTCC
1060	GGAGGGCATCCTGTGTTCCACGTTCC
1046.75	GGAGGGCATCCTGAATTCCACGCGCC

Table S4.1 continued

1041.875	GGAGGGCATCCTGATTTCCACGTTCC
1041.75	GGAGGGCATCCTGAATTCCACGTTCC
1018.5	GGAGGGCATCCTGGTTTCCACGCACC
989.125	GGAGGGCATCCTGGTTTCCACGTCCC
968.875	GGAGGGCATCCTGGGTTCCACACGCC
965.75	GGAGGGCATCCTGGTTTCCACTTACC
921.125	GGAGGGCATCCTGGGTTCCACTTCCC
915.25	GGAGGGCATCCTGGTTTCCACGTGCC
883.5	GGAGGGCATCCTGAGTTCCACTTGCC
856.625	GGAGGGCATCCTGTGTTCCACTTTCC
853	GGAGGGCATCCTGAATTCCACTTCCC
849.125	GGAGGGCATCCTGAGTTCCACTTTCC
834.25	GGAGGGCATCCTGGGTTCCACAGTCC
822.625	GGAGGGCATCCTGAATTCCACGTCCC
788.5	GGAGGGCATCCTGTATTCCACTCACC
786.625	GGAGGGCATCCTGTATTCCACGTTCC
784.625	GGAGGGCATCCTGAATTCCACGAACC
784.125	GGAGGGCATCCTGGTTTCCACTCTCC
757.75	GGAGGGCATCCTGTATTCCACTGACC
752.375	GGAGGGCATCCTGGATTCCACTCGCC
737	GGAGGGCATCCTGGGTTCCACATGCC
697.25	GGAGGGCATCCTGTATTCCACTCTCC
685	GGAGGGCATCCTGTTTTCCACTCTCC
675.5	GGAGGGCATCCTGGCTTCCACTGTCC
673.25	GGAGGGCATCCTGGATTCCACTGCCC

Table S4.1 continued

650.875	GGAGGGCATCCTGAGTTCCACTGCCC
616.125	GGAGGGCATCCTGGGTTCCACGGACC
610.625	GGAGGGCATCCTGAGTTCCACCTGCC
610.5	GGAGGGCATCCTGGATTCCACGTGCC
599	GGAGGGCATCCTGGTTTCCACCTTCC

```
#!/usr/bin/perl -w
#use strict;


my $infilename = $ARGV[0];
my $outfilename = $ARGV[1];

my $lookfor = "GGAGGGCATCCTG..TTCCAC...CC";

# Open the file.
open(INFILE, $infilename) or die "Cannot open $ARGV[0]: $!.\n";
open(OUTFILE, '>', $outfilename) or die "no out file input. $!.\n";

# read every line
while(my $line = <INFILE>) {
        $match = false;
        my $i = 0;
        my $ii = 0;
        my $iii = 0;
        my $match = false;


        for($i = 0; $i < length($line);$i++){
                $outline = "";
                $ii = 0;
                my $match1 = substr($line,$i,1);
                my $match2 = substr($lookfor,$ii,1);
```

Figure S4.1: Perl script used to search for P1•P2-5N from the Hiseq runs. Raw data had to be filtered and sequences put into a single column before the script was run.

```
                if($match1 eq $match2){

                        for($i;$i < length($line); $i++){
                                $iii = $i;

                                $match1 = substr($line,$i,1);
                                $match2 = substr($lookfor,$ii,1);

                                if($match2 eq "."){$outline .= substr($line,$i,1);}
                                else {

                                        if($match1 eq $match2) { $outline .=
substr($line,$i,1);}
                                        else { $match = false;$i = $iii; last;}
                                }

                                if($ii >= length($lookfor)) {$match = false; last;}
                                if(substr($lookfor,length($lookfor) - 1,1) eq
substr($line,$i,1)){
                                        if( $ii == length($lookfor) - 1) {$match = true;
print OUTFILE "$outline\n";last;}
                                }

                                $ii++;
                        }
                }

        }
}

close INFILE;
close OUTFILE;
```

Figure S4.1 continued

CHAPTER 5

DNAZYME LIGATION IN ICE

Ribozymes have had a longer history compared to DNAzymes (DNA enzymes). The first ribozymes were first discovered in the early 1980's, by Altman's group working on RNase P in *E. coli*, and Cech's group working on rRNA splicing in *Tetrahymena thermophila* (Kruger et al. 1982, Guerrier-Takada et al. 1983). The work on these ribozymes would later lead to the Nobel Prize in Chemistry for being the first to discover the catalytic properties of RNA. Since then there have been many examples of natural catalytic RNAs: the hammerhead ribozyme (Prody et al. 1986, Hutchins et al. 1986), hairpin ribozyme from the tobacco ringspot virus (Hampel and Tritz 1989, Feldstein et al. 1989), self-splicing Group I introns (Cech 1990), and the *glmS* ribozyme that can both catalyze the production of glucosamine-6-phosphate and self-cleavage (Winkler et al. 2004) among several. In contrast, the first DNAzyme was first found in 1994 and only through *in vitro* selection. It could cleave a single RNA linkage embedded in the DNA sequence, with Pb^{2+} as cofactor, and claiming a 10^5 fold rate over spontaneous RNA cleavage (Breaker and Joyce 1994) (Figure 5.1). Since this first discovery, there have been more RNA-cleaving DNAzymes from *in vitro* selection experiments with varying functions including a biosensor for lead ions (Li and Lu 2000), repair enzyme for thymine dimers in DNA (Daniel and Dipankar 2004), and even as a nanomaterial for use in nanowires, nanoarchitectures and computing (Ito and Fukusaki 2004). The metal cofactor requirements for these have a wide range from Mg^{2+} (Breaker and Joyce 1995), Zn^{2+} (Li et al. 2000), Mn^{2+} (Cruz et al. 2004), Cu^{2+} (Liu and Lu 2007), the amino acid histidine (Roth and Breaker 1998), to no cofactor (Geyer and Sen 1997).

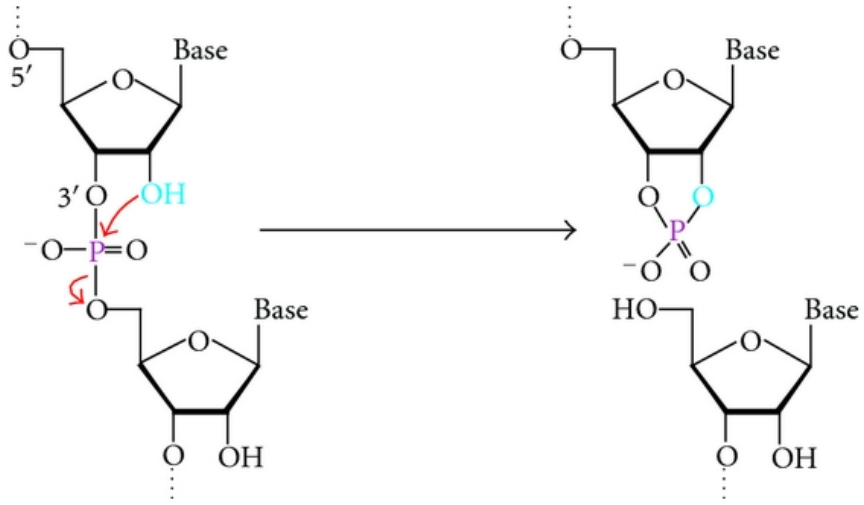

Figure 5.1 Cleavage of RNA catalyzed by both ribozymes and DNAzymes. The cleavage products is 2'3' -cyclic phosphate and a 5' -OH (Reprinted from Tram et al. 2012)

Although all known DNAzymes were artificially selected and have yet to be found in nature, this does not preclude DNA from being a contender as a biomolecule in a self-replicating system on early Earth. There are many examples of cleaving DNAzymes, but what about ligation? DNAzymes can ligate both RNA and DNA (Cuenoud and Szostak 1995, Sreedhara et al. 2004, Liu and Lu 2007, Purtha et al. 2005). One type of DNA ligase forms a new phosphodiester bond between a 5' -OH and a 3' -phosphorimidazolide (Cuenoud and Szostak 1995) and another DNAzyme requires an AppDNA oligo and a 3'OH on the other oligo (Sreedhara et al. 2004). As for RNA ligation, *In vitro* selection has generated many DNA sequences that can form a 3'-5' linkage between two RNA substrates possessing a 2'3' -diol on one and a 5' triphosphate on the other (Figure 5.2). The requirement for a high energy nucleoside triphosphate makes this reaction unlikely for early Earth (Keefe and Miller 1995).

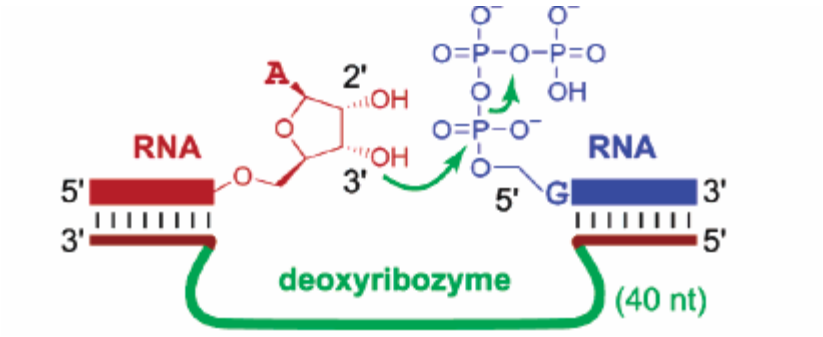

Figure 5.2: RNA-ligating DNAzyme with a 40nt core region with binding arms for the two RNA substrates. One RNA substrate must possess a 2'3' -diol, the other a 5' triphosphate (Reprinted from Purtha et al. 2005)

Both RNA cleavage reactions of the DNAzyme and the ribozyme generate a 2'3'-cyclic phosphate and a 5'-OH (Figure 5.1). Cleaved products can ligate back to full length RNA substrate by increasing the ligation rate in frozen solution, perhaps this is true for the RNA cleaving DNAzymes as well. The DNAzymes tested are variants of two motifs: the 8-17 and the 10-23 (Figure 5.3). These motifs have different secondary structure, cleavage/ligation site requirements, and solution condition requirements for efficient cleavage (Santoro and Joyce 1997, Cruz et al. 2004).

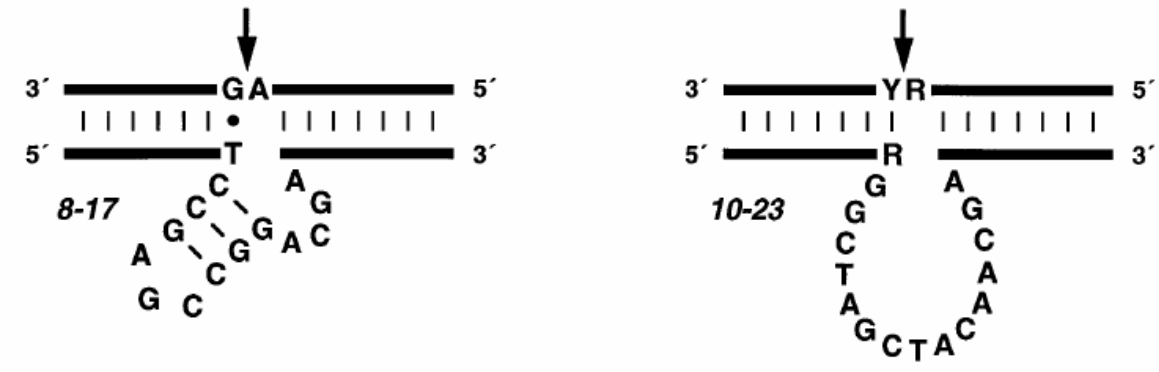

Figure 5.3: Secondary structures of 8-17 and 10-23 DNAzyme motifs with substrate requirements. 8-17 requires A and G in the dinucleotide junction for efficient cleavage. 10-23 cleaves between an R (purine A or G) and Y (pyrimidine U or C) (Reprinted from Santoro and Joyce 1997).

Methods and Materials

RNAs and DNAs

All RNAs and DNAs were ordered from Integrated DNA Technologies (IDT), Iowa. Each pair of DNAzyme/RNA substrate with an attached 6-fluorescein amidite targeted a specific dinucleotide junction cleavage site (Table 5.1). **A*A**: 5'- GAA ACT TGC TTA AGC AAG AAG CAT GTC AGT GAC TCG AA A AAA AAT TCG TTA 3'/ 5' UAA CGA AUU UUU UA*A GUG CUU CUU GCU UAA GCA AGU UUC -6-FAM 3'; **A*C**: 5'- AAA TTC G GGCTAGCTACAACGA T ACA CCA GGA AAT CTG ATG TGT T -3'/ 5' AAC ACA UCA GAU UUC CUG GUG UAA CGA AUU U -6-FAM 3'; **A*G**: 5'- GAA ACT TGC TTA AGC AAG AAG CA T GTC AGC GAC ACG AA TA AAA AAT TCG TTA -3'/ 5' UAA CGA AUU UUU UAA* GUG CUU CUU GCU UAA GCA AGU UUC -6-FAM 3'; **A*U**: 5' GGC GAG TGG AAG GCT AGC TAC AAC GAC CAG GAT GCC CTC C 3'/ 5'GGA GGG CAU CCU GGA* UUC CAC UCG CC -8-FAM 3'; **C*A**: 5'- AAA TTC GTT ACA CCA GGA AAT C GTC AGCT GAC TCGAA ATG TGT T -3'/ 5' AAC ACA UC*A GAU UUC CUG GUG UAA CGA AUU U -6-FAM 3'; **C*C**: 5'- AAA TTC GTT ACA CCA T GTC AGC GAC ACG AA A AAT CTG ATG TGT T -3'/ 5' AAC ACA UCA GAU UUC* CUG GUG UAA CGA AUU U -6-FAM 3'; **C*G**: 5'- AAA TT T GTC AGC GAC ACG AA TT ACA CCA GGA AAT CTG ATG TGT T -3'/ 5' AAC ACA UCA GAU UUC CUG GUG UAA C*GA AUU U -6-FAM 3'; **C*U**: 5'- AAA TTC GTT ACA CCA GGCTAGCTACAACGA GA AAT CTG ATG TGT T -3'/ 5' AAC ACA UCA GAU UUC C*UG GUG UAA CGA AUU U -6-FAM 3'.

DNAzyme Ligation

1 µM of each DNAzyme that contains the 10-23 core region was annealed to 1 µL of substrate RNA by heating to 90 ^{o}C in 100 µL of 50 mM Tris pH 7.5, 150 mM NaCl for 2 min before $MgCl_2$ was added to a final concentration of 10 mM and then incubated at 37 ^{o}C for 1 hour. Similarly for the 8-17 variants, 1 µM DNAzyme and 1 µM of the appropriate RNA substrate was heated to 90 ^{o}C in 100 µL of 50 mM HEPES pH 7.0, 100 mM KCl, 400 mM NaCl for 2 min, before the addition of 7.5 mM $MgCl_2$ and 7.5 mM $MnCl_2$ and subsequent incubation at 23 ^{o}C for 1 hour.

This heating and cooling was repeated five more times for complete cleavage. 10 µL aliquots were removed, quick-frozen with a -80 ^{o}C ethanol bath, and incubated at the indicated temperatures. Reactions were halted by adding a stopping solution of deionized formamide and 20 mM EDTA with bromophenol blue and xylene cyanol in a 4:1 volume ratio to the sample. Products were run on a 12% denaturing polyacrylamide gel (7 M urea) and analyzed with an Alpha Imager and Fuji Multi Gauge Imaging software.

Results

DNAzyme Ligation of P1 and P2

We tested RNA-cleaving DNAzymes on eight of the 16 possible dinucleotide junctions. The DNAzyme motif chosen for each junction is based on a DNAzyme's observed preferences on a cleavage site. The substrates are all natural sequences with the designated dinucleotide in the RNA. Of the eight DNAzyme/RNA pair, only one demonstrated ligation (Table 5.1).

Table 5.1: Dinucleotide junctions with associated DNAzyme/RNA substrate pair. Only one of the 8 pairs showed successful ligation.

Dinucleotide Junction Target	DNAzyme motif	RNA substrate	Demonstrated Ligation
A*A	8-17, variant E2112	DsrA domain II	N
A*C	10-23	DsrA domain I	N
A*G	8-17, variant E1111	DsrA domain II	N
A*U	10-23	P1-P2 of Schist26	Y
C*A	8-17, variant E5112	DsrA domain I	N
C*C	8-17, variant E1111	DsrA domain I	N
C*G	8-17, variant E1111	DsrA domain I	N
C*U	10-23	DsrA domain I	N

The 10-23 DNAzyme motif is able to ligate the dinucleotide junction A*U using its own cleavage reaction buffer, with only one difference: a different incubation temperature. The incubation temperature used for cleavage is 37 °C, but cooling the solution changes the equilibrium constant, increasing the ligation rate compared to the cleavage rate (Figure 5.4A). Freezing the solution achieves the highest ligation yield of 31% at both -10 °C and -15 °C, but ice formation is not strictly necessary since some ligation occurs even if the solution remains in liquid phase at -10 °C (Figure 5.4B).

A B

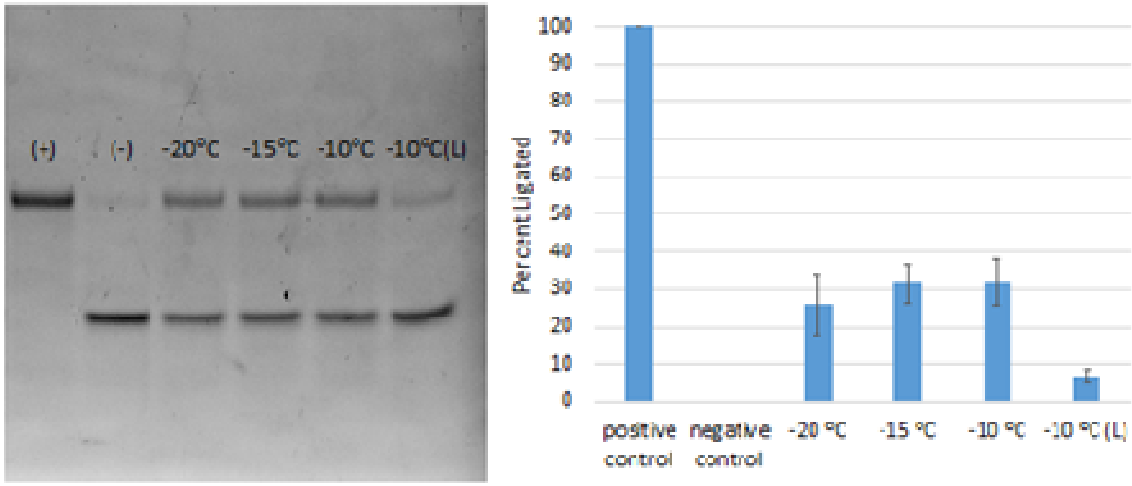

Figure 5.4: DNAzyme motif 10-23 ligating the P1•P2 RNA of the Schist26 hammerhead ribozyme. A) 12% PAGE 7M Urea separating the full length FAM6-labeled P1•P2 (+) from the cleaved product (-). B) Graph of ligation yield at different temperatures. Freezing does not appear to be necessary, but it does enhance ligation (31% at -10 °C) compared to supercooled (7% at -10 °C). Data represents at least three replicates with standard deviation as error bars.

Effect of buffer and pH

The standard cleavage/ligation buffer includes 50 mM Tris pH 7.5 with 150 mM NaCl. If the pH deviates from 7.5, the ligation yield (31%) suffers and drops to less than 20% at pH 7.0 and about 25% at pH 8.0 (Figure 5.5). Carboxylates have been shown to increase the freeze-induced ligation yield of the Schist26 hammerhead ribozyme (Chapter 3), and we wondered if this may be true for the 10-23 DNAzyme. Replacing 150 mM NaCl with tri-sodium citrate did not show ligation products at pH 7.0, but increasing the pH eventually brought its ligation yield to comparable numbers to the standard solution. We replaced Tris with another common buffer: HEPES. There was no significant difference in ligation yield between pH 7.0 and 8.0, but overall it did better than Tris, reaching 40% (Figure 5.5). Percent yield for the three conditions tested appears to increase as the buffer approaches pH 8.0, if Tris's pH is adjusted for low temperatures. In Chapter 3, Tris at pH 8.0 at 25 °C, increases by 1 at -20 °C. The temperatures are not the same here, but it does indicate that pH 8.0 in Figure 5.5 has a higher value at -15 °C.

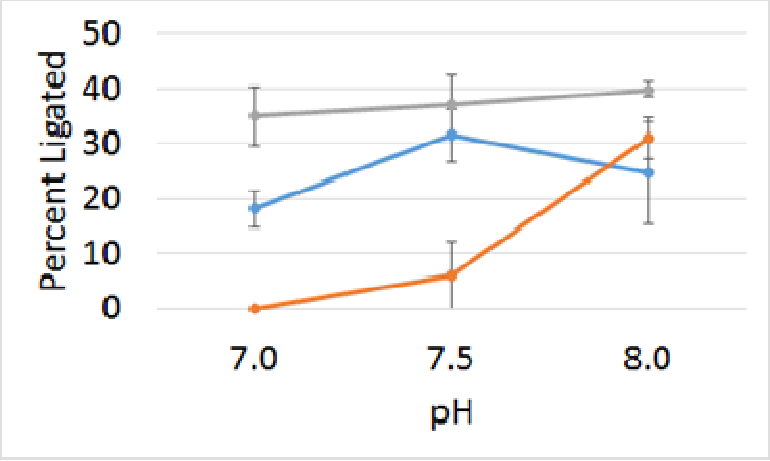

Figure 5.5: Plot of 10-23 DNAzyme ligation at different buffer conditions, frozen at -15 °C. Blue line is the standard 50 mM Tris with 150 NaCl. Orange uses 50 mM Tris with

150 tri-sodium citrate and the gray line is 50 mM HEPES with 150 NaCl.

Discussion

The RNA World hypothesis has had many decades to accumulate functional ribozymes, providing more and more support that RNA, not DNA or protein, was the key biomolecule for a self-replicating system. Catalytic RNAs have many functions, but among them is cleavage and ligation of RNA substrates, important processes for generating complexity and diversity in RNA sequences.

As for DNAzymes, the first ones to be discovered were RNA-cleaving and generated a 5'-OH and 2'3'-cyclic phosphate, similar products to many RNA-cleaving ribozymes (Breaker and Joyce 1994). RNA-ligating DNAzymes were eventually discovered, but required a 5'-triphosphate and a 2'3'-diol. The work presented here demonstrates a simpler system for ligation, without the high-energy polyphosphate as a substrate requirement. Because the RNA-cleaving DNAzymes generate similar products like the hairpin and hammerhead ribozymes, they may ligate these two cleaved substrates back together. This ligation reaction was achieved in ice for the hairpin ribozyme by Vlassov et al. in 2004 and for the hammerhead ribozyme in Chapter 3.

Of all the DNAzymes tested, only one showed observable ligation (Table 5.1). The 10-23 DNAzyme ligated well in a 1:1:1 ratio of enzyme to both substrates, up to 40%. Although the other DNAzyme/RNA substrate pairs did not show observable ligation, does not mean they are incapable of ligation. The protocol requires almost complete cleavage of the full length RNA substrates by the DNAzyme to generate the cleaved RNA products needed for ligation. Many of the enzymes could not cleave half of the RNA despite repeated cycles of heating and annealing. If ligation occurred, it was indistinguishable from the uncleaved full length RNA substrate.

CHAPTER 6

CONCLUSION

We can never know how life started, but we can always propose ideas on how it may have started. One of these is the RNA World Hypothesis. It suggests that RNA is the likeliest candidate in early self-replicating systems (Woese 1967, Orgel 1968, and Crick 1968). Chapter 2 widens the RNA World to include the possibility of Fe^{2+} in RNA catalysis. Chapters 3 and 4 argue for a cold and dry RNA World. Chapter 5 is meant to expand the RNA World, not challenge it. DNAzymes and ribozymes may have coexisted, cleaving and ligating themselves and each other.

Most of the chapters have no clear practical application, except for Chapter 5. The DNAzymes tested can potentially be base paired to any RNA sequence and cleave at specific sites, like using a restriction enzyme for specific DNA sequences. The only requirement is choosing the right DNAzyme motif and designing the DNAzyme binding arms to be complementary to the target RNA. Ligation, the other side of the reversible cleavage reaction, also holds that potential. This can allow the ligation of specific RNAs in a pool of other RNAs, eliminating the need for extraction and purification beforehand.

Growing the Ribosomal RNA

Both cleavage and ligation reactions on RNA is important for the RNA World, this back and forth process can generate new and diverse sequences. Here we combine the major themes of this thesis to propose how the complexity in ribosomal RNA may have evolved.

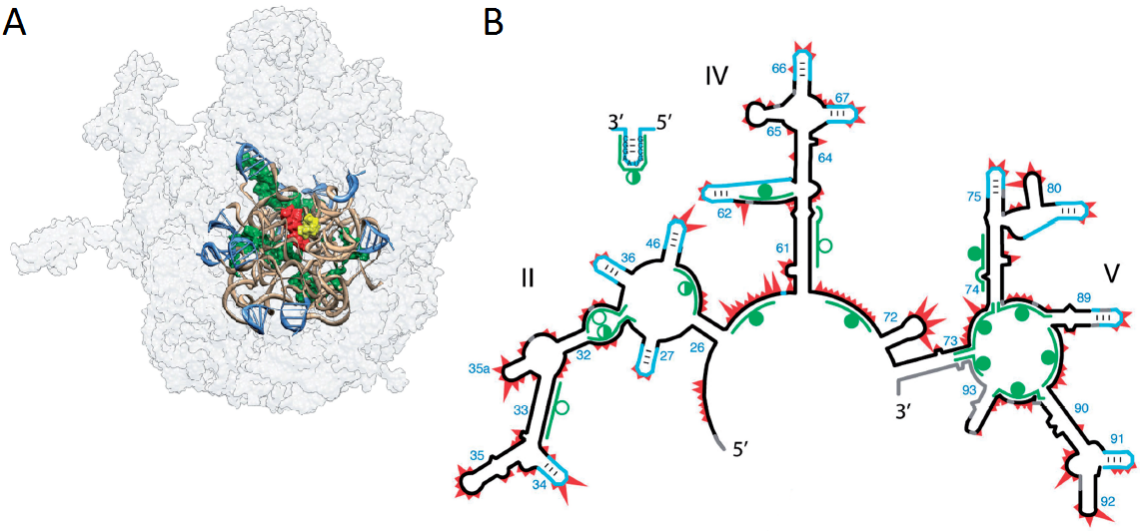

Figure 6.1: Model of the a-PTC. A) The 3-D model of the ~ 60 Å in diameter a-PTC over the watermark of the LSU. B) Secondary structure of the a-PTC as proposed by SHAPE and RNAse H digestion assay (Adapted from Hsiao et al. 2013).

The ribosome is one of biology's most important processes, responsible for translating RNA to proteins. The large subunit (LSU) of the ribosome contains the peptidyl transferase center (PTC), the site of catalysis for peptide bonds, and is believed to be the oldest part of the ribosome. A model for a truncated LSU with sections of the 23S rRNA, ribosomal peptides, and divalent cations was designed to preserve the catalytic activity and then called the ancestral (a-PTC) (Hsiao et al. 2013). This model reduced the ~3000 nucleotide 23S rRNA to 615 nucleotides (Figure 6.1). Although this was a considerable reduction in size, the rRNA can be further broken down into phases, each composed of a set of insertion fingerprints and ancestral expansion segments (AES). As the oldest region of the rRNA, Phase 1 and 2 represented the PTC with AES 1 to 5 (Petrov et al. 2014). Figure 6.2 exhibits the insertion fingerprint site on the AES 1 where it will be expanded by AES 2. Although this model provides a step by step series of rRNA insertions and expansions, it does not show how the rRNA acquired them.

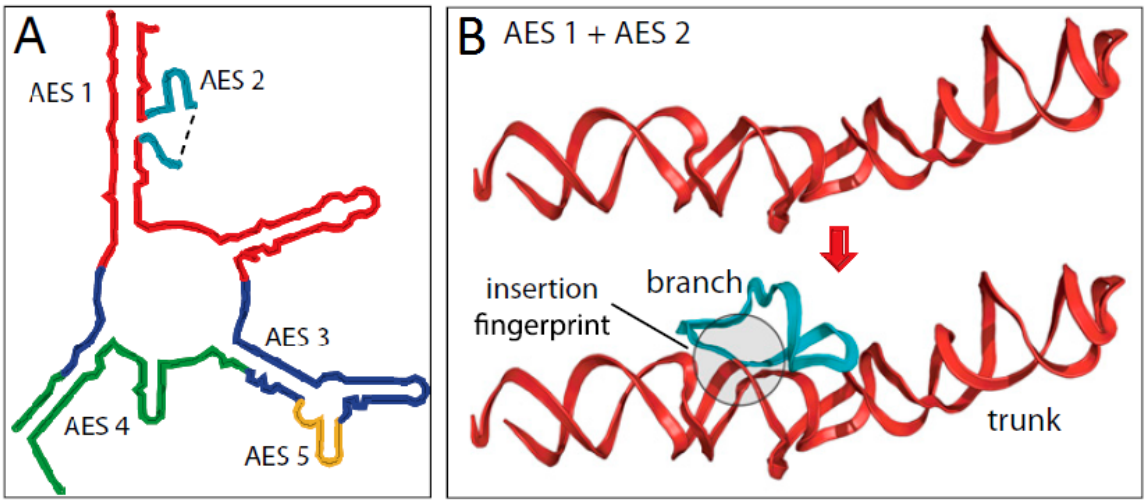

Figure 6.2: Ribosomal RNA evolution with insertion fingerprints and ancestral expansion segments (AES). A) Peptidyl transferase center color coded into AES 1 to 5. B) AES 1 is expanded by AES 2 from the insertion fingerprint site (Adapted from Petrov et al. 2014).

Lutay et al. demonstrated in 2007 the non-enzymatic recombination of RNA using simple RNA oligos O1 and O2. Dangling non-base paired poly(A) ends of the O1 RNA can be degraded by metal-induced cleavage, leaving a 2'3'-cyclic phosphate available for ligation to the neighboring RNA strand possessing a 5' –OH, leading to the product O1-O1 without the poly(A) tail (Figure 6.3). Replication of this non-enzymatic recombination produced two ligation products: one band about 26 nt, presumably the O1-O1 product with a tail of AAAA, and another about 22 nt with no poly(A) tails (Figure 6.4). This recombination is inefficient even after 7 days of incubation with 5 mM $MgCl_2$.

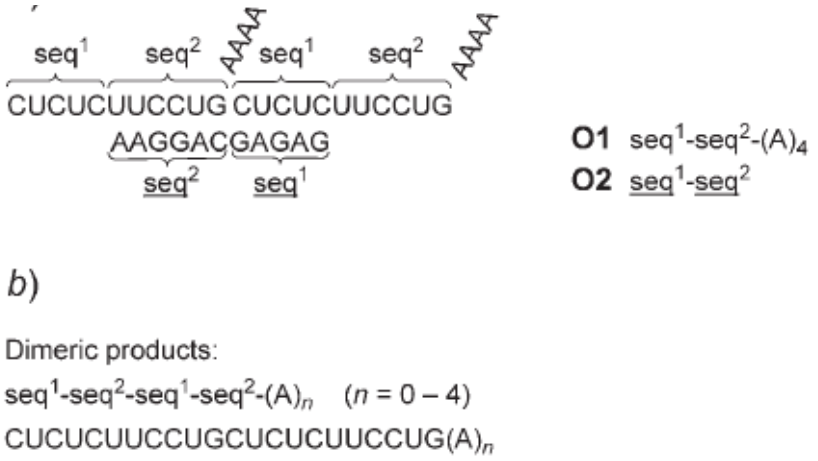

Figure 6.3: Predicted duplex formation of O1 and O2 RNA oligos. A) Nonenzymatic recombination of RNA occurs when the poly(A) tail of O1 is degraded, leaving a 2'3'-cyclic phosphate at the end of seq^2 and then ligation between the seq^2 and seq^1. B) The 26nt product is the result of the ligation of two O1 oligos with one poly(A) tail (Reprinted from Lutay et al. 2007).

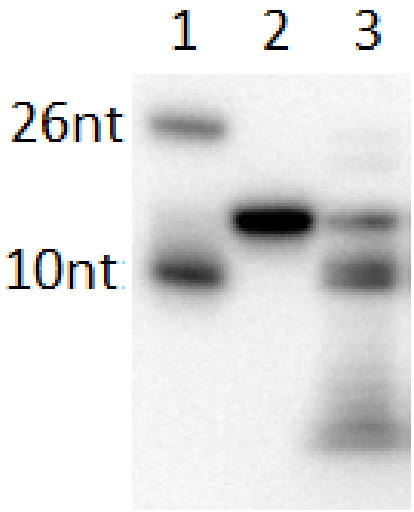

Figure 6.4: 12% PAGE replicating the non-enzymatic recombination of RNA oligos done by Lutay et al. 2007. Lane 1 is ^{32}P-labeled 26nt and 10nt RNA. Lane 2 contains the ^{32}P-labeled 16nt O1 RNA oligo. Lane 3 contains the ^{32}P-labeled O1 and non-labeled O2 in bis-tris-propane pH 9.0, 5 mM $MgCl_2$, at 37 °C for 7 days.

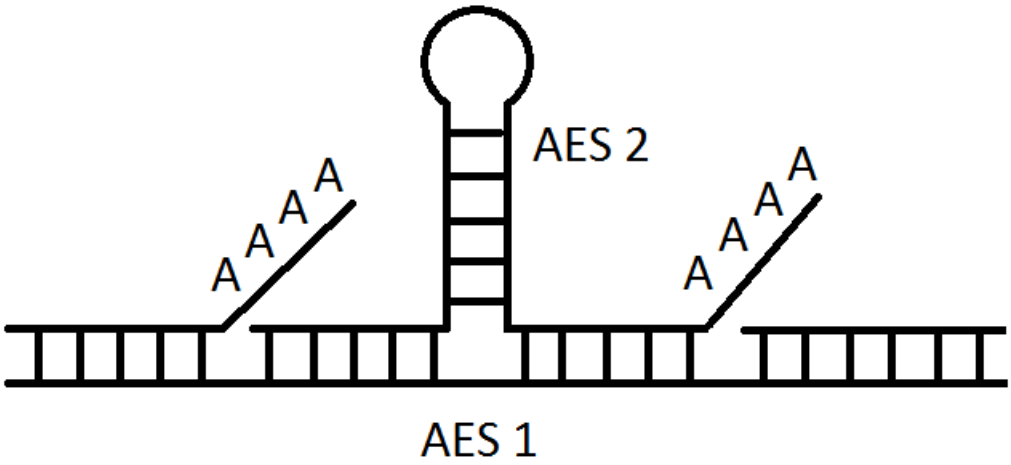

Figure 6.5: Non-enzymatic RNA recombination of AES 1 to include AES 2. Poly(A) tail will degrade, leaving a 2'3' –cyclic phosphate to ligate to the 5' –OH of the adjacent strand.

This non-enzymatic RNA recombination can be applied to ribosomal evolution. A spontaneous nick in AES 1 can open the area for AES 2 to base pair (Figure 6.5). Ligation of AES 2 into AES 1 completes the recombination. The divalent metal cation used to induce cleavage is Mg^{2+}, but perhaps using Fe^{2+} will enhance the recombination yield.

A second method for recombination is through DNAzymes (Figure 6.6). DNAzymes can cleave at specific sites on the AES 1, generating a 2'3'-cyclic phosphate and 5'OH. AES 2 can insert into the nicked AES 1 and be ligated by other DNAzymes. If recombination is done with freeze-induced ligation, the DNAzymes that cleaved AES 1 can be the same ones that ligate, if DNAzymes demonstrate similar reduced sequence requirements observed for Schist26 hammerhead enzyme in Chapter 4.

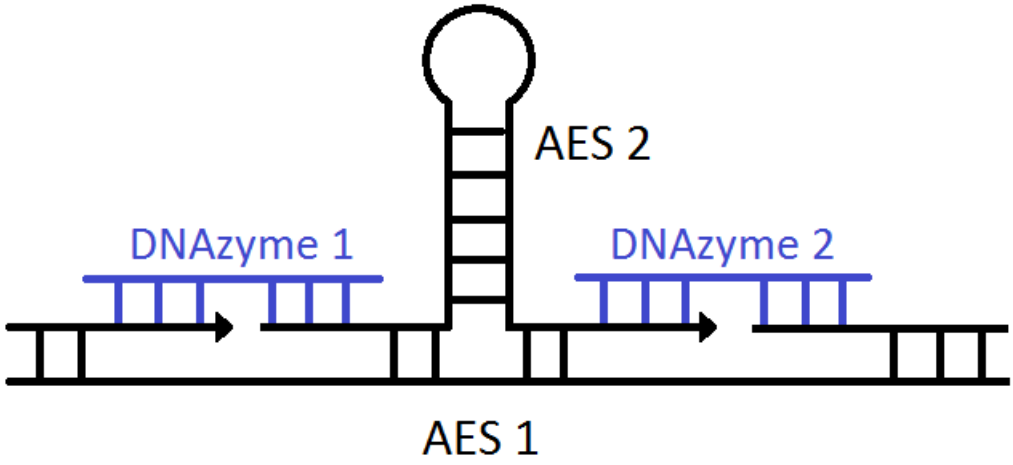

Figure 6.6: AES 2 ligating into AES 1 by DNAzymes. Ligation can be preceded by cleavage by DNAzymes as well.

REFERENCES

Adamala K, Szostak JW. 2013. Nonenzymatic template-directed RNA synthesis inside model protocells. Science 342: 1098-1100.

Aird D, Ross MG, Chen WS, Danielsson M, Fennell T, Russ C, Jaffe DB, Nusbaum C, Gnirke A. 2011. Analyzing and minimizing PCR amplification bias in Illumina sequencing libraries. Genome Biol 12.

Anderson M, Schultz EP, Martick M, Scott WG. 2013. Active-Site Monovalent Cations Revealed in a 1.55-angstrom-Resolution Hammerhead Ribozyme Structure. J Mol Biol 425: 3790-3798.

Attwater J, Wochner A, Pinheiro VB, Coulson A, Holliger P. 2010. Ice as a protocellular medium for RNA replication. Nat Commun 1.

Auffinger P, Grover N, Westhof E. 2011. Metal ion binding to RNA. Metal ions in life sciences 9: 1-35.

Bada JL. 2004. How life began on earth: a status report. Earth and Planetary Science Letters 226: 1-15.

Bada JL, Lazcano A. 2002. Origin of life. Some like it hot, but not the first biomolecules. Science 296: 1982-1983.

Biondi E, Maxwell AW, Burke DH. 2012. A small ribozyme with dual-site kinase activity. Nucleic Acids Res 40: 7528-7540.

Birikh KR, Heaton PA, Eckstein F. 1997. The structure, function and application of the hammerhead ribozyme. European journal of biochemistry / FEBS 245: 1-16.

Breaker RR, Joyce GF. 1994. A DNA enzyme that cleaves RNA. 1994. Chemistry and Biology 1:223-229.

Breaker RR, Joyce GF. 1995. A DNA enzyme with Mg^{2+}-dependent RNA phosphoesterase activity. Chemistry and Biology 2:655-660.

Canny MD, Jucker FM, Kellogg E, Khvorova A, Jayasena SD, Pardi A. 2004. Fast cleavage kinetics of a natural hammerhead ribozyme. J Am Chem Soc 126: 10848-10849.

Canny MD, Jucker FM, Pardi A. 2007. Efficient ligation of the Schistosoma hammerhead ribozyme. Biochemistry 46: 3826-3834.

Cech TR. 1990. Self-splicing of group I introns. Annu Rev Biochem 59: 543-568.

Chi YI, Martick M, Lares M, Kim R, Scott WG, Kim SH. 2008. Capturing hammerhead ribozyme structures in action by modulating general base catalysis. Plos Biol 6: 2060-2068.

Clark C. 2003. The physics of ice cream. Physics Education 38: 248-253.

Collins KD. 2006. Ion hydration: Implications for cellular function, polyelectrolytes, and protein crystallization. Biophysical chemistry 119: 271-281.

Crick F. 1970. Central Dogma of Molecular Biology. Nature 227: 561-563.

Cruz RPG, Withers JB, Li Y. 2004. Dinucleotide Junction Cleavage Versatility of 8-17 Deoxyribozyme. Chemistry and Biology 11:57-67.

Cuenoud B, Szostak JW. A DNA metalloenzyme with DNA ligase activity. 1995. Nature 375: 611-614.

Curtis EA, Bartel DP. 2001. The hammerhead cleavage reaction in monovalent cations. Rna 7: 546-552.

Darnell J. 2011. RNA: Life's Indispensable Molecule. Cold Spring Harbor Laboratory Press.

De la Pena M, Gago S, Flores R. 2003. Peripheral regions of natural hammerhead ribozymes greatly increase their self-cleavage activity. Embo J 22: 5561-5570.

De la Pena M, Garcia-Robles I. 2010. Ubiquitous presence of the hammerhead ribozyme motif along the tree of life. Rna 16: 1943-1950.

Endo M, Hirata K, Ihara T, Sueda S, Takagi M, Komiyama M. 1996. RNA hydrolysis by the cooperation of carboxylate ion and ammonium ion. J Am Chem Soc 118: 5478-5479.

Emilsson GM, Nakamura S, Roth A, Breaker RR. 2003. Ribozyme speed limits. RNA 9: 907-918.

Fedor MJ. 2009. Comparative Enzymology and Structural Biology of RNA Self-Cleavage. Annu Rev Biophys 38: 271-299.

Feldstein PA, Buzayan JM, Bruening G. 1989. Two sequences participating in the autolytic processing of satellite tobacco ringspot virus complementary RNA. Gene 82: 53-61.

Ferris JP, Hill AR, Jr., Liu R, Orgel LE. 1996. Synthesis of long prebiotic oligomers on mineral surfaces. Nature 381: 59-61.

Fishbaugh KE, Lognonné P, Des Marais DJ, Korablev O, Raulin F, Lognonné P, , Korable O. 2007. *Geology and Habitability of Terrestrial Planets*. Springer Science pg 63.

Forster AC, Symons RH. 1987. Self-cleavage of virusoid RNA is performed by the proposed 55-nucleotide active site. Cell 50: 9-16.

Geyer CR, Sen D. 1997. Evidence for the metal-cofactor independence of an RNA phosphodiester-cleaving DNA enzyme. Chemistry and Biology 4:579-593.

Gilbert W. 1986. Origin of Life - the Rna World. Nature 319: 618-618.

Guerrier-Takada C, Gardiner K, Marsh T, Pace N, Altman S. 1983. The RNA moeity of ribonuclease P is the catalytic subunit of the enzyme. Cell 35: 849-857.

Hammann C, Luptak A, Perreault J, de la Pena M. 2012. The ubiquitous hammerhead ribozyme. Rna 18: 871-885.

Hampel A, Tritz R. 1989. RNA catalytic properties of the minimum (-)sTRSV sequence. Biochemistry 28: 4929-4933.

Han J, Burke JM. 2005. Model for general acid-base catalysis by the hammerhead ribozyme: pH-activity relationships of G8 and G12 variants at the putative active site. Biochemistry 44: 7864-7870.

Hertel KJ, Herschlag D, Uhlenbeck OC. 1994. A Kinetic and Thermodynamic Framework for the Hammerhead Ribozyme Reaction. Biochemistry 33: 3374-3385.

Hertel KJ, Herschlag D, Uhlenbeck OC. 1996. Specificity of hammerhead ribozyme cleavage. Embo J 15: 3751-3757.

Higashi K, Terui Y, Suganami A, Tamura Y, Nishimura K, Kashiwagi K, Igarashi K. 2008. Selective Structural Change by Spermidine in the Bulged-out Region of Double-stranded RNA and Its Effect on RNA Function. J Biol Chem 283: 32989-32994.

Hsiao C, Lenz TK, Peters JK, Fang PY, Schneider DM, Anderson EJ, Preeprem T, Bowman JC, O'Neill EB, Lie L, Athavale SS, Gossett JJ, Trippe C, Murray J, Petrov AS, Wartell RM, Harvey SC, Hud NV, Williams LD. 2013. Molecular Paleontology: A Biochemical Model of the Ancestral Ribosome. Nucleic Acids Res 41: 3373-3385.

Hsiao C, Chou IC, Okafor CD, Bowman JC, O'Neill EB, Athavale SS, Petrov AS, Hud NV, Wartell RM, Harvey SC, Williams LD. 2013. RNA with Iron(II) as a cofactor catalyses electron transfer. Nature chemistry 5: 525-528.

Hutchins CJ, Rathjen PD, Forster AC, Symons RH. 1986. Self-Cleavage of Plus and Minus Rna Transcripts of Avocado Sunblotch Viroid. Nucleic Acids Res 14: 3627-3640.

Johnston WK, Unrau PJ, Lawrence MS, Glasner ME, Bartel DP. 2001. RNA-catalyzed RNA polymerization: accurate and general RNA-templated primer extension. Science 292: 1319-1325.

Joyce GF. 1989. RNA evolution and the origins of life. Nature 338: 217-224.

Kanavarioti A, Monnard PA, Deamer DW. 2001. Eutectic phases in ice facilitate nonenzymatic nucleic acid synthesis. Astrobiology 1: 271-281.

Kazakov SA, Balatskaya SV, Johnston BH. 1998. Freezing-induced self-ligation of the hairpin ribozyme: Cationic effects. Structure, Motion, Interaction and Expression of Biological Macromolecules, Vol 2: 155-161.

Kazakov SA, Balatskaya SV, Johnston BH. 2006. Ligation of the hairpin ribozyme in cis induced by freezing and dehydration. Rna 12: 446-456.

Khvorova A, Lescoute A, Westhof E, Jayasena SD. 2003. Sequence elements outside the hammerhead ribozyme catalytic core enable intracellular activity. Nat Struct Biol 10: 708-712.

Kruger K, Grabowski PJ, Zaug AJ, Sands J, Gottschling DE, Cech TR. 1982. Self-splicing RNA: autoexcision and autocyclization of the ribosomal RNA intervening sequence of Tetrahymena. Cell 31: 147-157.

Lambert D, Draper DE. 2007. Effects of osmolytes on RNA secondary and tertiary structure stabilities and RNA-Mg2+ interactions. J Mol Biol 370: 993-1005.

Lee DH, Granja JR, Martinez JA, Severin K, Ghadiri MR. 1996. A self-replicating peptide. Nature 382: 525-528.

Levy M, Miller SL. 1998. The stability of the RNA bases: implications for the origin of life. Proceedings of the National Academy of Sciences of the United States of America 95: 7933-7938.

Li J, Zheng W, Kwon H, Lu Y. 2000. *In vitro* selection and characterization of a highly efficient Zn(II)-dependent RNA-cleaving deoxyribozyme. Nucleic Acids Res 28: 481-488.

Li YF, Breaker RR. 1999. Kinetics of RNA degradation by specific base catalysis of transesterification involving the 2 '-hydroxyl group. J Am Chem Soc 121: 5364-5372.

Liu J, Lu Y. 2007. Colorimetric Cu2+ detection with a ligation DNAzyme and nanoparticles. Chem Commun 46: 4872-4874.

Lutay AV, Zenkova MA, Vlassov VV. 2007. Nonenzymatic Recombination of RNA: Possible Mechanism for the Formation of Novel Sequences. Chem Biodiversity 4: 762-767.

Martick M, Scott WG. 2006. Tertiary contacts distant from the active site prime a ribozyme for catalysis. *Cell* 126: 309-320.

Mulkidjanian AY, Bychkov AY, Dibrova DV, Galperin MY, Koonin EV. 2012. Origin of first cells at terrestrial, anoxic geothermal fields. PNAS: E821-E830.

Murray JB, Seyhan AA, Walter NG, Burke JM, Scott WG. 1998. The hammerhead, hairpin and VS ribozymes are catalytically proficient in monovalent cations alone. Chemistry & biology 5: 587-595.

Nelson JA, Shepotinovskaya I, Uhlenbeck OC. 2005. Hammerheads Derived from sTRSV show enhanced cleavage and ligation rate constants. Biochemistry 44: 14577-14585.

O'Rear JL, Wand S, Feig AL, Beigelman L, Uhlenbeck OC, Herschlag D. 2001. Comparison of the hammerhead cleavage reactions stimulated by monovalent and divalent cations. RNA 7: 537-545.

Pace NR. 1991. Origin of life--facing up to the physical setting. Cell 65: 531-533.

Penedo JC, Wilson TJ, Jayasena SD, Khvorova A, Lilley DM. 2004. Folding of the natural hammerhead ribozyme is enhanced by interaction of auxiliary elements. RNA 10:880-888.

Perreault J, Weinberg Z, Roth A, Popescu O, Chartrand P, Ferbeyre G, Breaker RR. 2011. Identification of hammerhead ribozymes in all domains of life reveals novel structural variations. PLoS computational biology 7: e1002031.

Petrov AS, Bernier CR, Hsiao C, Norris AM, Kovacs NA, Waterbury CC, Stepanov VG, Harvey SC, Fox GE, Wartell RM, Hud NV, Williams LD. 2014. Evolution of the ribosome at atomic resolution. PNAS 111: 10251-10256.

Prody GA, Bakos JT, Buzayan JM, Schneider IR, Bruening G. 1986. Autolytic Processing of Dimeric Plant-Virus Satellite Rna. Science 231: 1577-1580.

Prousek J. 2007. Fenton Chemistry in biology and medicine. Pure Appl Chem 79: 2325-2338.

Renz M, Lohrmann R, Orgel LE. 1971. Catalysts for Polymerization of Adenosine Cyclic 2',3'-Phosphate on a Poly (U) Template. Biochim Biophys Acta 240: 463-&.

Reuter JS, Mathews DH. 2010. RNAstructure: software for RNA secondary structure prediction and analysis. BMC bioinformatics 11: 129.

Roth A, Breaker RR. 1998. An amino acid as a cofactor for a catalytic polynucleotide. 1998. Proceedings of the National Academy of Sciences of the United States of America 95: 6027-6031.

Roy S. 2008. Cleavage and ligation studies in hairpin and hammerhead ribozymes using site specific nucleotide modifications. Vol PhD. University of Vermont, Burlington, VT.

Sanchez R, Ferris J, Orgel LE. 1966. Condition for purine synthesis: Did prebiotic synthesis occur at low temperatures?. Science 153: 72-73.

Sambrooks J, Russell DW. 2001. *Molecular Cloning*. Cold Spring Harbor Laboratory Press, New York, pg A1.3.

Sawai H, Wada M. 2000. Nonenzymatic template-directed condensation of short-chained oligouridylates on a poly(A) template. Orig Life Evol Biosph 30: 503-511.

Seidell A, Linke WF. 1958. Solubilities of Inorganic and Metal Organic Compounds. Princeton, NJ: Van Nostrand.

Serganov A, Patel DJ. 2009. Amino acid recognition and gene regulation by riboswitches. Bba-Gene Regul Mech 1789: 592-611.

Stage-Zimmermann TK, Uhlenbeck OC. 2001. A covalent crosslink converts the hammerhead ribozyme from a ribonuclease to an RNA ligase. Nat Struct Biol 8: 863-867.

Sulston J, Lohrmann R, Orgel LE, Miles HT. 1968. Nonenzymatic synthesis of oligoadenylates on a polyuridylic acid template. Proc Natl Acad Sci 59: 726-733.

Sun X, Li JM, Wartell RM. 2007. Conversion of stable RNA hairpin to a metastable dimer in frozen solution. Rna 13: 2277-2286.

Trinks H, Schroder W, Biebricher CK. 2005. Ice and the origin of life. Origins of life and evolution of the biosphere: the journal of the International Society for the Study of the Origin of Life 35: 429-445.

Turk RM, Chumachenko NV, Yarus M. 2010. Multiple translational products from a five-nucleotide ribozyme. Proceedings of the National Academy of Sciences of the United States of America 107: 4585-4589.

Uhlenbeck OC. 1987. A small catalytic oligoribonucleotide. Nature 328: 596-600.

Vlassov AV, Johnston BH, Landweber LF, Kazakov SA. 2004. Ligation activity of fragmented ribozymes in frozen solution: implications for the RNA world. Nucleic Acids Res 32: 2966-2974.

Vlassov AV, Kazakov SA, Johnston BH, Landweber LF. 2005. The RNA world on Ice: A new scenario for the emergence of RNA information. J Mol Evol 61: 264-273.

Winkler WC, Nahvi A, Roth A, Collins JA, Breaker RR. 2004. Control of gene experssion by a natural metabolite-responsive ribozyme. Nature 428: 281-286.

Wolf AV. 1966. Aqueous solutions and body fluids; their concentrative properties and conversion tables. Hoeber Medical Division, New York.

Yusupov MM, Yusupova GZ, Baucom A, Lieberman K, Earnest TN, Cate JH, Noller HF. 2001. Crystal Structure of the ribosome at 5.5 A resolution. Science 292: 883-896.

VITA

LIVELY LIE

Lively Lie was born in Jakarta, Indonesia. She attended schools in Jakarta and then Alpharetta and Lilburn, Georgia. She received a B.A. in Biology from Georgia Institute of Technology in 2007 before pursuing a doctorate in Biology. In her free time, she enjoys annoying her husband Sergio, playing computer games, drawing and reading.